Design of a Vertical-Axis Wind Turbine

Final Report

4 April 2014

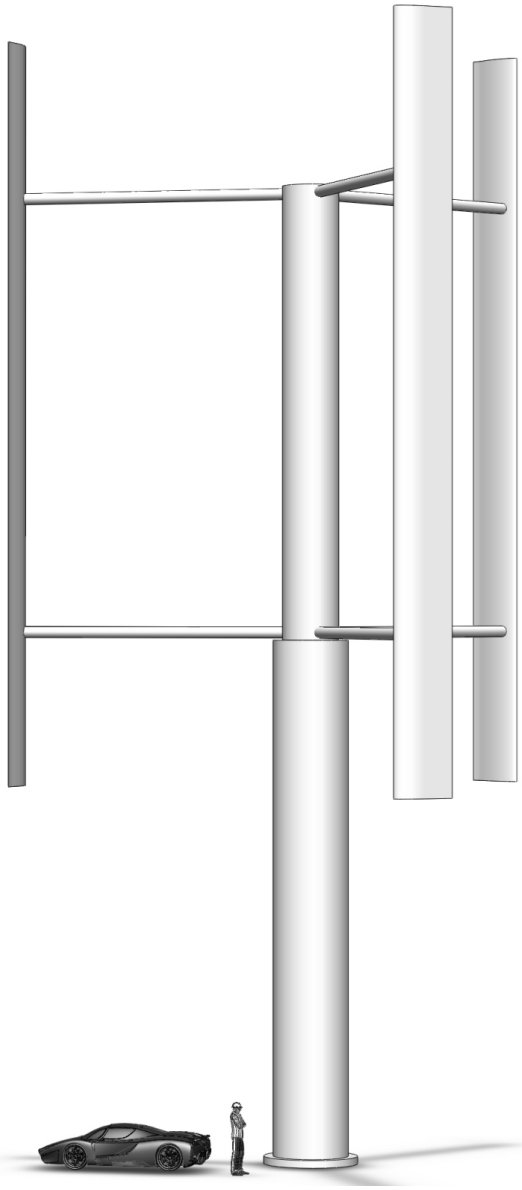

MUN VAWT Design Group M11
Jonathan Clarke
Luke Hancox
Daniel MacKenzie
Matthew Whelan

Abstract

This report created by MUN VAWT Design highlights the design of a Vertical-Axis Wind Turbine (VAWT) for application in remote communities in Newfoundland and Labrador. The goal is for this VAWT to produce enough energy to provide substantial reduction in fuel consumption by diesel generators in these communities. Enclosed is the structural design, aerodynamics simulation results, basic vibrational analysis, mechanical component design and a brief economic analysis. Aerodynamic simulations were completed using Q-Blade and CFD modeling, further analysis was recommended to include 3D CFD modeling. Structural design involved various components including the blades, struts, hub and tower. Mechanical components are related to inner rotational parts, such as bearings, couplings, and driveshafts. The economic analysis was extrapolated from cost reports from the Northern Power 100 horizontal-axis wind turbines (HAWT) found in Ramea, NL.

Acknowledgements

We would like to thank everyone who helped us realize this project including:

Dr. Luc Rolland – Project Supervisor

Dr. Samer Nakhla – Provided guidance with structural and composites design

Dave Parsons – Provided guidance with selection of mechanical components

Table of Contents

List of Figures

List of Tables

List of Equations

1 Introduction

In remote regions of Canada that are not connected to the electrical grid, communities and industries typically rely on diesel generators to meet their power requirements. However, rising fuel costs and continuing deficiencies in infrastructure and transportation make alternatives to diesel attractive. A potential means to reduce reliance on diesel is the use of wind turbines in conjunction with conventional generators.

The vertical-axis turbine configuration offers some advantages for this application. Vertical-axis wind turbines (VAWTs) are generally simpler mechanically than a horizontal-axis type because they do not require any yawing mechanism to keep them pointed into the wind. In addition, the gearbox (if one is required) and generator are located at the bottom of the tower, making maintenance and repair easier. These features provide significant advantage in remote locations where spare parts may not be readily available.

2 Project Goals

2.1 Target Application

As electronic devices continue to grow in popularity, so does our need for energy. To reduce the negative effect that increasing power consumption will have on the environment, it is an engineering responsibility to continuously develop and improve ways to produce green, renewable energy. Many models of VAWTs have been developed in the past, but the target will be remote communities and industrial sites. These areas are generally off-grid and are supplied with energy by means of diesel generators.

2.2 Design Constraints

MUN VAWT Design has taken on the task of designing a feasible vertical-axis wind turbine for remote communities and industrial sites of Newfoundland and Labrador, and other places with similar climates. The design will meet the following constraints:

- Work in conjunction with diesel generators instead of replacing them
- Simple in design to reduce manufacturing costs and maintenance issues
- Able to produce sufficient energy to offset fuel costs
- Can be shipped to remote areas via aircraft or boat

2.3 Scope

With respect to designing the turbine, MUN VAWT Design researched existing wind turbines, airfoil structures, Newfoundland and Labrador weather data and energy consumption of remote communities and industrial sites in Canada. Computational fluid dynamics and SolidWorks models were completed. A website was created to showcase the design and provide project updates. The group also tracked the progress of the project with a Gantt chart and project plan accepted by the Faculty of Engineering at Memorial University of Newfoundland.

The project examined the following aspects of the VAWT design:

- Detailed structural design and analysis
- Detailed aerodynamic simulation using computational fluid dynamics
- Basic vibrational analysis
- Selection of various off the shelf components
- Modelling and engineering drawings of mechanical and structural components
- Economic analysis

MUN VAWT Design did not focus on designing a structural foundation or connecting to the power grid.

3 Research

3.1 Benefits of VAWT Design

Vertical-axis wind turbines offer several advantages over more conventional horizontal-axis wind turbines (HAWTs) with regards to reliability, practicality and noise concerns. The first major advantage is that they can operate from winds travelling in any direction.

Therefore, a yaw system is not required to change the orientation of the turbine blades based on the direction of the wind. The lack of a yaw system increases the reliability of the wind turbine while decreasing its capital costs. [1] Second, VAWTs are easier to maintain since the generator and drivetrain components are located at the base of the structure. VAWTs also generate less noise than HAWTs; areoacoustic analysis has shown that the unsteady flow caused by cyclic variation of VAWT blade velocities reduces the radiated sound. [2] Finally, VAWTs are well suited for offshore environments. The heavy equipment of a VAWT associated with power generation, namely the transmission and the generator, is mounted below the rotor. This configuration permits a low center of gravity and the ability to place these components at or below sea level. This provides additional stability to the structure that supports the rotor while reducing its capital costs. [1]

3.2 Weather Data

Historical data for weather conditions in the target area was acquired from Environment Canada. A detailed analysis of data from Nain, Newfoundland and Labrador in the period from September 2012 to September 2013 was carried out to determine typical conditions and allow for proper sizing of the turbine. This data was compared with samples from other years and locations to verify that it is typical. Wind speed data at the Nain weather station is recorded at an elevation of 7.6 metres above sea level. Since a medium-sized turbine will most likely exceed this height, the recorded speeds were extrapolated up to 30 metres above sea level using the wind gradient equation [3]:

Equation 1: Wind Gradient Equation

$$V_{30} = V_{7.6}\left({h_{30}}/{h_{7.6}}\right)^{a}$$

Where V is the wind speed, h is the elevation, and a is the Hellman exponent describing the shape of the wind gradient.

Statistical analysis of the wind data at 7.6 metres elevation shows an average speed of 5.2 m/s, and a maximum of 27.2 m/s. Corrected to 30 metres elevation, this corresponds to an average of 6.4 m/s and a maximum of 33 m/s [4].

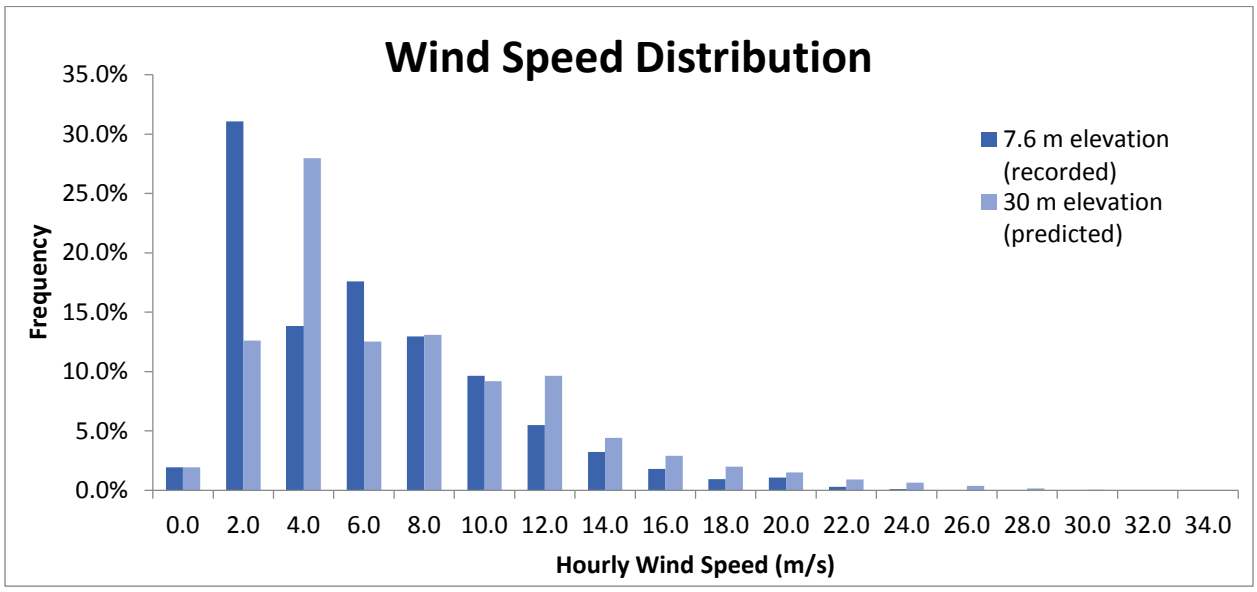

Figure 1: Histogram of Wind Speed Data for Nain, Labrador

The average speed varies based on season, with the highest speeds being recorded in winter and fall. This is advantageous, since highest power demand in the target region typically occurs during those seasons. [5]

Table 1: Wind Speed Statistics by Season for Nain, Labrador

WIND SPEED STATISTICS										
Season	**Year**		**Winter**		**Spring**		**Summer**		**Fall**	
Elevation (metres)	7.6	30	7.6	30	7.6	30	7.6	30	7.6	30
Average Speed (m/s)	5.24	6.37	5.89	7.17	4.79	5.83	4.30	5.24	5.98	7.28
Median Speed (m/s)	4.17	5.07	5.28	6.42	4.17	5.07	3.61	4.39	5.28	6.42
Maximum Speed (m/s)	27.22	33.12	27.22	33.12	20.56	25.01	17.50	21.29	24.17	29.40

Records of wind gusts were also available. The largest gusts are usually in the vicinity of 35 m/s, or 120 km/h, and occur in the winter.

3.3 Sizing

VAWTs are sized based on power requirements and wind speed. MUN VAWT Design is developing a VAWT that will produce energy in conjunction with diesel generators in remote communities and industrial sites. Through research it was determined that on average a Canadian home consumes 3.8kW in January and 1.4kW in August, with an average wind speed of 6.4 m/s at 30 meters elevation. [5] [4] In order to maintain a reasonable size for shipping purposes, the turbine will be sized at 100kW. An individual turbine will be able to power approximately 25 homes at maximum generating capacity and power consumption. This will not entirely replace diesel generators, but will mitigate fuel consumption by implementing a renewable energy source and to keep up with growing electricity demands.

3.4 Literature Review

In order to evaluate the feasibility of the project, a variety of VAWT projects were examined to find the existing research. In the 1980's, FloWind Corporation commercialized full-Darrieus wind turbines based on research conducted at Sandia National Laboratories. 17m and 19m turbines rated at 142 and 250 kW respectively were developed and generated a peak of 100 million kWh in 1987. These early Darrieus turbines suffered from fatigue failure related to the blade manufacturing method. The joints between the sections of extruded aluminum blades failed leading to the eventual bankruptcy of FloWind. [6].

Figure 2: FloWind Full-Darrieus VAWT

A 2006 study by Eriksson et. al compared four different designs of wind turbines. The first was the VAWT 850, a 500kW VAWT made in the UK. The second was a modified version of the 850 using a different tower design. The third design was the 500kW Sandia Darrieus turbine built in the 1980's. The final design was a HAWT constructed by Siemens rated at 600kW with the data scaled down to 500kW using Froude scaling. The table below shows their resulting comparison. Their conclusions stated that the second H-rotor is a potential competitor to a HAWT and suggested improvements by making lighter support arms and using a three bladed design.

Table 2: Technical Specifications for Various Configurations

A comparison of technical specifications for different turbines

	H-rotor 1	H-rotor 2	Darrieus	HAWT (scaled)	HAWT
Rated power (kW)	500	500	500	500	600
Swept area (m^2)	850	850	955	1370	1520
Rated wind speed (m/s)	~13.5	~13.5	12.5	15	15
No. of blades	2	2	2	3	3
Tower height (m)	30	30	50	47	50
Turbine diameter (m)	35	35	34	42	44
Blade length (m)	24.3	24.3	54.5	18	19
Blade material	GRP	GRP	Aluminium	GRP	GRP
Yaw mechanism	No	No	No	Yes	Yes
Pitch or active stall mechanism	No	No	No	Yes	Yes
Gear box	Yes	No	Yes	Yes	Yes
Guy wires	No	No	Yes	No	No
Generator position	In tower	On ground	On ground	In nacelle	In nacelle
Rotation speed (rpm)	Constant, 13.6/20.4	Variable	Semi-variable, 28–38	Constant, 19/28	Constant, 18/27
Overall structure	Simple	Simple	Moderate	Complicated	Complicated
Mass blades only (t)	6	6	-	13	15
Mass turbine (t)	~24	~24	72.2	13	15
Mass nacelle (t)	~20	No nacelle	No nacelle	20	23
Mass tower (t)	153	32.8	No tower	36	42
Total weight above ground level (t)	197	56.8	72.2	68	80

In order to use a Darrieus turbine effectively, the type of airfoil is very important. Many VAWTs in the past relied on the NACA symmetric series with the NACA 0018 being a popular choice. Using the NACA 0018 as a starting point, Delft University of Technology master's student M. C. Claessens developed the DU 06-W-200. The following table highlights the differences between the NACA 0018 and the DU 06-W-200 airfoils. [7]

Table 3: NACA 0018 vs. DU 06-W-200 Airfoils

NACA 0018	DU 06-W-200
Turbulent	Laminar
18% Thickness	20% Thickness
Symmetric	0.8% Camber

There are several benefits to using the DU 06-W-200 airfoil. First, the extra thickness increases the blade strength without decreasing the performance. Also, the DU 06-W-200 has a much higher $C_{L,max}$ for positive angles of attack which results in lower drag. Lastly, stall occurs at higher angles of attack with a smaller drop in lift coefficient.

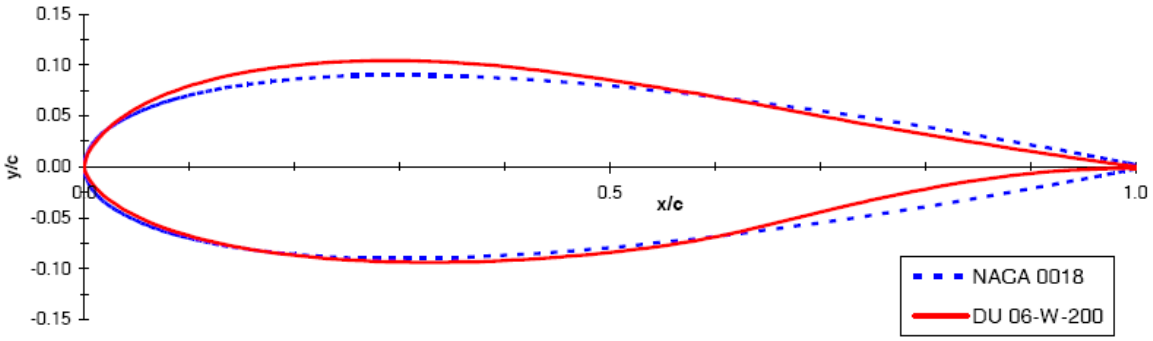

Figure 3: Visual comparison of NACA 0018 and DU 06-W-200 airfoils

4 Concept Selection

4.1 Preliminary Design

For the preliminary design, several VAWT design options were considered based on existing research. It was determined that using existing research was preferable to generating concepts through group brainstorming since the group had little experience with VAWT design. A large amount of academic and industry-based research exists concerning the design of vertical-axis wind turbines; this provided a solid starting point for

the group's design. The overall design was split up into 4 categories: VAWT configuration, number of blades, airfoil type and solidity.

4.2 VAWT Configurations

The two most common types of VAWTs are the Darrieus and Savonius configurations. Darrieus wind turbines have lift-based aerofoils around a rotating shaft while Savonius turbines have drag-based "scoops" around a rotating axis. Due to the higher efficiency and lower weight of the Darrieus configuration, it was chosen over the Savonius counterpart for the preliminary design. The Darrieus wind turbine has several sub-configurations including the full-Darrieus (or eggbeater), the "H" and the "V" configurations.

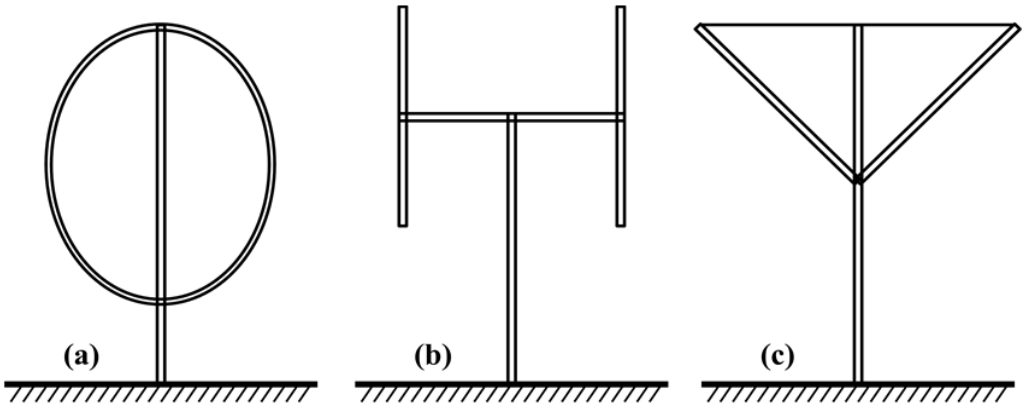

Figure 4: Darrieus VAWT Configurations

The "H-Darrieus" configuration was selected as it combines the high efficiency of a Darrieus turbine with the simplicity of the "H" configuration.

4.3 Number of Blades

The number of blades on a Darrieus-type VAWT has a significant effect on the stability, efficiency and cost. Initial research showed that 2-bladed and 3-bladed configurations were the most common although 4-bladed configurations were also considered. 2-bladed VAWTs have lower capital costs since they use fewer materials; however, 3-bladed VAWTs allow for a reduction in the size of the tower, bearings, and foundation, thereby offsetting the cost

of the additional blade. Two-bladed VAWTs generate symmetric loadings that contribute to the in-plane and out-of-plane vibrational modes of the rotor. With a 3-bladed VAWT, there are no in-plane or out-of-plane rotor vibrational modes resulting in greater rotor stability. In addition, the third blade reduces torque ripple in the rotor's torque output, thus reducing vibrations and noise while increasing reliability. [1] The following graph shows how the power coefficient (C_P) changes with respect to the blade tip speed ratio for different numbers of blades (adapted from "Determination of Vertical Axis Wind Turbines Optimal Configuration through CFD Simulations"):

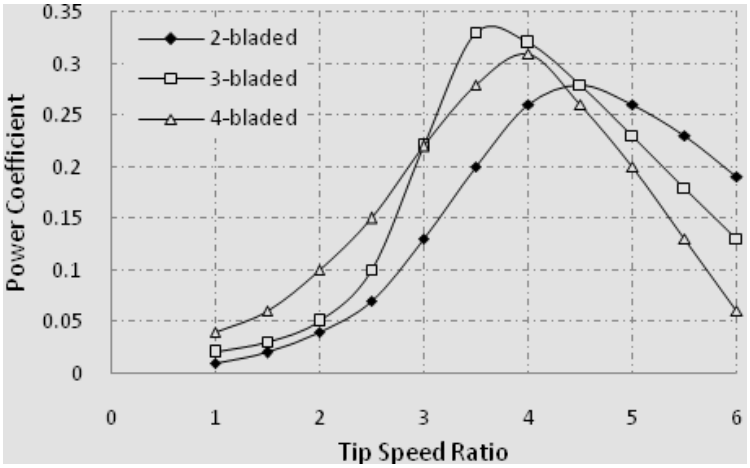

Figure 5: Performance Curve of "H-Darrieus" VAWT Based on Number of Blades

A 3-bladed VAWT design was selected since it increases rotor stability, eliminates symmetrical loading, reduces torque ripple in the drive train, and the experimental results of Sabaeifard et al. for 3-bladed designs were favourable. [8]

4.4 Airfoil Selection

The following graph shows how the power coefficient (C_P) changes with respect to the blade tip speed ratio for different airfoils with error bars (adapted from "Determination of Vertical Axis Wind Turbines Optimal Configuration through CFD Simulations"):

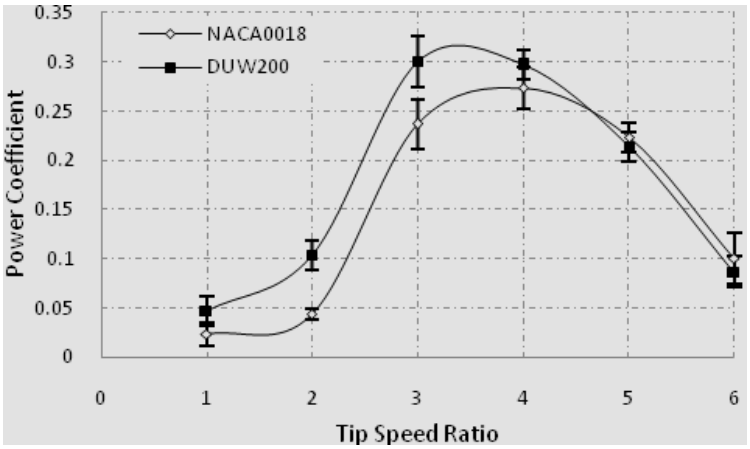

Figure 6: Performance Curve of "H-Darrieus" VAWT with Different Airfoils

A DU 06-W-200 airfoil (shortened to DUW200 in the above graph) was selected since the experimental results of Sabaeifard et al. for the DU 06-W-200 airfoil were more favourable than for the conventional NACA airfoil. [8]

4.5 Solidity

The following graph shows how the power coefficient (C_P) changes with respect to the blade tip speed ratio for different solidity values (adapted from "Determination of Vertical Axis Wind Turbines Optimal Configuration through CFD Simulations"):

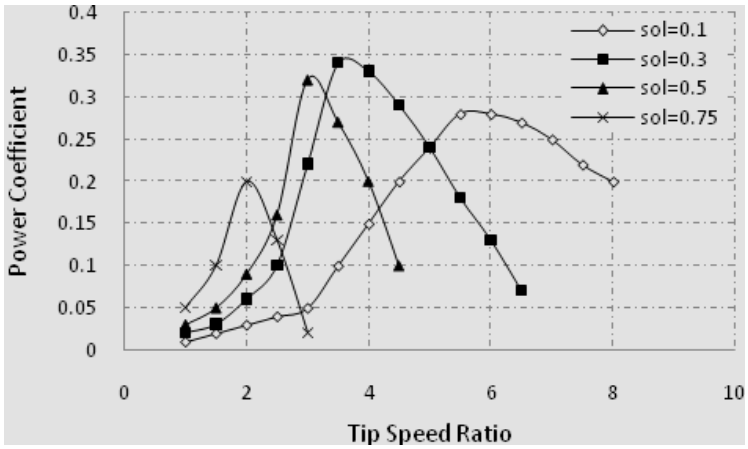

Figure 7: Performance Curve of "H-Darrieus" VAWT with Different Solidity Values

From the above graph, a solidity value between 0.3 and 0.5 would provide ideal results. From the graph and additional experimental results of Sabaeifard et al., a solidity of 0.35 was selected. [8]

4.6 Summary

The following table summarizes the preliminary design decisions that were made. The highlighted cells represent the decisions made by the group.

Table 4: Summary of Preliminary Design Decisions

Criteria	**Optimal Choice**	**Alternatives**
Configuration	H-Rotor Darrieus	Full Darrieus, V-Rotor Darrieus, Savonius
Number of Blades	3	2 to 5
Airfoil	DU 06-W-200	NACA-Series Airfoils
Solidity	0.35	0.15 to 0.5

5 Regulations and Standards

5.1 General

After completion of Phase I research into sizing and weather patterns, the standards and regulations that govern wind turbines were consulted. The standard chosen to consult was IEC 61400-1 titled Wind turbines – Part 1: Design Requirements, developed by the International Electrotechnical Commission (IEC). The IEC is a worldwide organization for the standardization of all electrical, electronic and related technologies. The goal of the IEC is to "promote international co-operation on all questions concerning standardization in the electrical and electronics fields."

The purpose of this section of the IEC 61400 is to specify the minimum design requirements for wind turbines in order to ensure the engineering integrity of the turbine. It is not intended to be used as a complete specification or instruction manual but to provide the engineering and technical requirements to guarantee the safety of the

structural, mechanical, electrical, and control systems. The standard can be used for any size wind turbine but is not intended for the design of offshore turbines; small wind turbines are also subject to IEC 61400-2.

This standard covers all subsystems of the turbine including: control systems, protection mechanisms, internal electrical systems, mechanical systems and support structures. Also, the standard should be used in conjunction with other applicable standards where appropriate. Although the standard is concerned with requirements that apply to the design, manufacture, installation and manuals for operation and maintenance of a wind turbine and the associated quality management process the area of concern for the project is the design requirements set out in the standard. [9]

5.2 Classes

A turbine following this standard is required to meet one of two types of safety classes, normal and special. The normal safety class is comprised of nine different cases as seen in Table 1, which are based on wind speed and turbulence parameters. This is because wind conditions are the primary source of external conditions that will affect the structural integrity of a turbine and the multiple cases allow for a wide variety of sites for different conditions without being overly specific. These conditions are not meant for the offshore environment or severe storms such as hurricanes. The class seen in the table is for the special safety factor which is chosen by the designer and/or customer.

Table 5: Basic parameters for wind turbine classes

Wind Turbine Class	I	II	III	S
Vref (m/s)	50	42.5	37.5	Special
A Iref	0.16			
B Iref	0.14			
C Iref	0.12			

The desired class for the project to meet is IA, which represents the highest reference wind speed and turbulence intensity categories used. This allows the turbine designed herein to operate in the widest variety of environments. The Vref or reference wind speed refers to an extreme 10 minute average wind speed with a recurrence period of 50 years acting at the turbine hub height. Iref is the expected turbulence intensity squared at 15m/s wind speed, where turbulence is defined as a random deviation in the wind speed from the 10 minute average. By meeting this safety classification the turbine will have a minimum design life of 20 years. [9]

5.3 Design Load Cases

The verification of the design can be completed through calculation or full scale testing of a wind turbine. In order to meet the standard through calculations, the use of a structural dynamics model is required. This model shall be used to analyze a number of design load cases specified in the standard. These are the minimum cases that a turbine must be designed for and are presented in Table 2. The design load cases consist of a combination of normal and extreme external conditions acting at various phases of turbine operation that are likely to result in critical situations. The list of abbreviations used in Table 2 can be found in Appendix A.

Table 6: Design Load Cases

Design Situation	DLC	Wind Conditions	Other Conditions	Type of Analysis	Partial Safety Factors
1) Power Production	1.1	NTM Vin<Vhub<Vout	For extrapolation of extreme events	U	N
	1.2	NTM Vin<Vhub<Vout		F	*
	1.3	ETM Vin<Vhub<Vout		U	N
	1.4	ECD Vhub = Vr-2, Vr, Vr +2		U	N
	1.5	EWS Vin<Vhub<Vout		U	N
2) Power Production plus occurrence of fault	2.1	NTM Vin<Vhub<Vout	Control System fault or loss of electrical network	U	N
	2.2	NTM Vin<Vhub<Vout	Protection System or preceding internal electrical fault	U	A
	2.3	EOG Vhub = Vr ± 2 and Vout	External or internal electrical fault including loss of electrical network	U	A
	2.4	NTM Vin<Vhub<Vout	Control, protection, or electrical system faults	F	*

			including loss of electrical network		
3) Start up	3.1	NWP Vin<Vhub<Vout		F	*
	3.2	EOG Vhub = Vin, Vr ± 2 and Vout		U	N
	3.3	EDC Vhub = Vin, Vr ± 2 and Vout		U	N
4) Normal Shut down	4.1	NWP Vin<Vhub<Vout		F	*
	4.2	EOG Vhub = Vr ± 2 and Vout		U	N
5) Emergency shutdown	5.1	NTM Vhub = Vr ± 2 and Vout		U	N
6) Parked (Standing Still or idling)	6.1	EWM 50 year recurrence period		U	N
	6.2	EWM 50 year recurrence period	Loss of electrical network connection	U	N
	6.3	EWM 1 year recurrence period	Extreme yaw misalignment	U	N
	6.4	NTM Vhub < 0.7Vref		F	*
7) Parked and fault conditions	7.1	EWM 50 year recurrence period		U	A
8) Transport, assembly maintenance and repair	8.1	NTM Vmaint to be stated by manufacturer		U	T
	8.2	EWM 50 year recurrence period		U	A

Due to the nature of the project not all the design load cases listed are relevant to the design of the turbine herein. The following cases will be neglected: 2.1 thru 2.4, 6.2, 6.3, 7.1, 8.1 and 8.2. The majority of these are due to the fact that the electrical network and control systems, the transport, assembly, maintenance and repair fall outside of the scope of the project. Case 6.3 is neglected because a vertical-axis wind turbine does not feature a yaw system.

Brief definitions of the applicable cases are presented below:

- DLC 1.1 and 1.2 are for normal turbulence during normal operation.
- DLC 1.3 is for ultimate loading resulting from extreme turbulence conditions.
- DLC 1.4 and 1.5 are for transient cases that have been found to be critical events.
- DLC 3.1 thru 3.3 specify transient events for the period the turbine moves from a standstill to normal operation.
- DLC 4.1 and 4.2 are the opposite cases of DLC 3.1 and 3.2.

- DLC 5.1 is for the same operation as DLC 4.1 and 4.2 but under an emergency situation.
- DLC 6.1 for standstill or idling is evaluated under extreme wind and 6.4 is for normal turbulence.

The simulations of the design load cases are required to be run at least six times for a 10-min stochastic realization. However, case 5.1 requires a minimum of 12 simulations. Another requirement is that the first 5 seconds of data be neglected for turbulent studies because of the effect that initial conditions have on dynamic analyses. [9]

6 Aerodynamics

6.1 Preliminary Sizing

Preliminary sizing was conducted using the wind power density formula: [10]

Equation 2: Wind Power Density Formula

$$W/_{m^2} = 0.5 * \rho_{avg} * C_p * V^3$$

This formula allows for the calculation of power generated per square metre of turbine swept area given average air density ρ_{avg}, power coefficient C_p, and wind speed V. Using an estimated power coefficient of 0.4, preliminary sizing indicated that in order to develop the desired maximum output power of 100kW at a wind speed of 10.5 m/s, the swept area of the turbine would need to be approximately 320 m^2.

6.2 QBlade Analysis

Preliminary aerodynamic analysis was conducted using QBlade, an open-source wind turbine simulation software developed by a team at the Technical University of Berlin, Germany. The software is integrated with the airfoil simulation code XFoil (developed by Mark Drela at the Massachusetts Institute of Technology) to provide lift and drag polars for standard NACA airfoils and extrapolate them to 360° angle-of-attack. Using these polars,

QBlade can evaluate the performance of a vertical-axis wind turbine using the double-multiple streamtube model. [11]

6.2.1 The Double-Multiple Streamtube Model

The double-multiple streamtube model (DMS model) for a vertical-axis wind turbine is an algorithm that computes aerodynamic forces on the turbine blades, taking into account that the blades pass through the flow stream twice. The blades are considered to absorb energy from the flow once in the upstream side of turbine, and once in the downstream side.

Similar to the actuator disk theory, the DMS method applies conservation of momentum to the flow impinging on the turbine. The swept area of the turbine is divided into two sets of elements (streamtubes). For each of these streamtubes, momentum conservation is compared with the blade forces computed from lift and drag coefficients at all azimuth angles. The upstream side is evaluated separately from the downstream side, with the induced flow velocity at the exit of the upwind streamtubes being used as the inflow for the downwind streamtubes. [12]

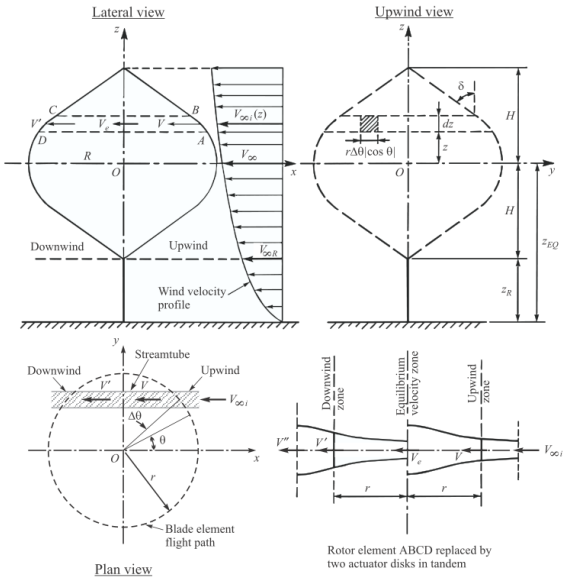

Figure 8: Discretization of VAWT for DMS method from the QBlade Guidelines [12]

Some limitations of this method identified by the software's developers include convergence issues for very high solidities and high tip-speed ratios. Since the turbine design is to have a moderate solidity of approximately 0.35, the solidity limitation was not

anticipated to cause any problems. The limitation on tip-speed ratio was avoided by prescribing the wind speed and turbine rotational speed for each simulation such that excessive tip-speed ratios were avoided. The software also neglects the effects of the wake of the support tower, and cannot account for dynamic stall of the turbine blades. Correction for these limitations is detailed in Section 3.5.

6.2.2 Turbine Evaluation

To perform preliminary evaluation of the turbine, a simple H-rotor-style VAWT was designed in QBlade with the specifications shown in Table 3. A variety of aspect ratios (ratio of blade height to rotor diameter) were evaluated to determine the configuration that gives the best power coefficient (the parameter that governs how much energy will be produced by the turbine in a given wind condition).

Table 7: Turbine Parameters

Configuration	1	2	3
Airfoil	DU06-W200	DU06-W200	DU06-W200
No. of Blades	3	3	3
Blade Chord	1.6 metres	1.6 metres	1.6 metres
Rotor Height	20 metres	17.9 metres	16 metres
Rotor Diameter	16 metres	17.9 metres	20 metres
Aspect Ratio	1.25 : 1	1 : 1	1 : 1.25

QBlade was used to generate plots of power coefficient vs. tip-speed ratio for the three configurations. From these results, the 1.25 : 1 aspect ratio gave the highest power coefficient and lowest tip-speed ratio at peak power coefficient. A low tip-speed ratio is considered desirable since high tip speeds are correlated to high levels of aerodynamic noise [10]. Higher aspect ratios may give higher power coefficients; however, it was decided to limit the height of the blades to 20 metres for ease of shipping.

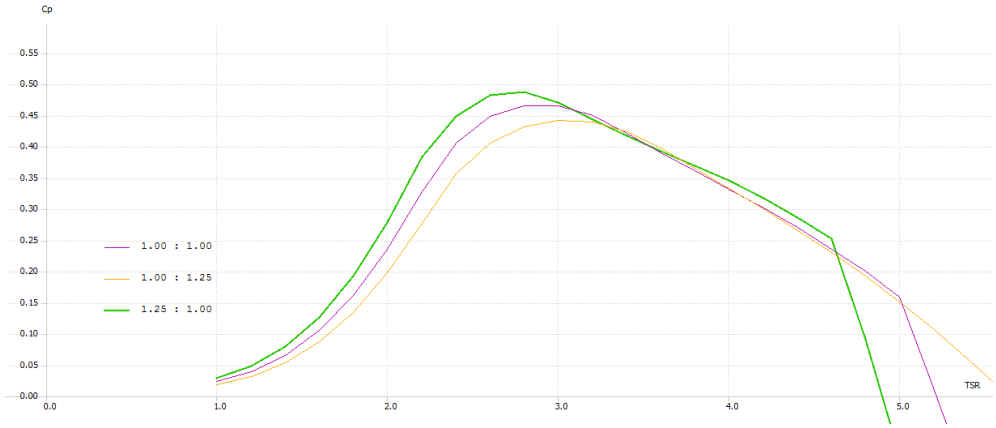

Figure 9: Power Coefficient vs. Tip-Speed Ratio for Various Aspect Ratios

6.2.3 Aerodynamic Results

To account for software limitations, an existing H-rotor turbine with known performance was modeled in QBlade to allow for comparison between experimental and theoretical data. The turbine used for this analysis was the VAWT 260. Developed in Great Britain in 1989, this experimental H-rotor turbine had a rated output of 100kW, a height of 13.3 metres, and a rotor diameter of 20 metres [13] [14]. By modelling this turbine in QBlade and comparing the results with experimental data, it was found that the software overestimated power coefficient by approximately 20%. Therefore, a correction factor was applied to the calculated power coefficient as follows:

Equation 3: Power Coefficient Equation

$$C_{p-corrected} = C_{p-raw} * \eta_{correction} * \eta_{generator}$$

Where $\eta_{correction} = 0.8$ and $\eta_{generator}$ is assigned a typical value of 0.96. The corrected power coefficient plot is shown below.

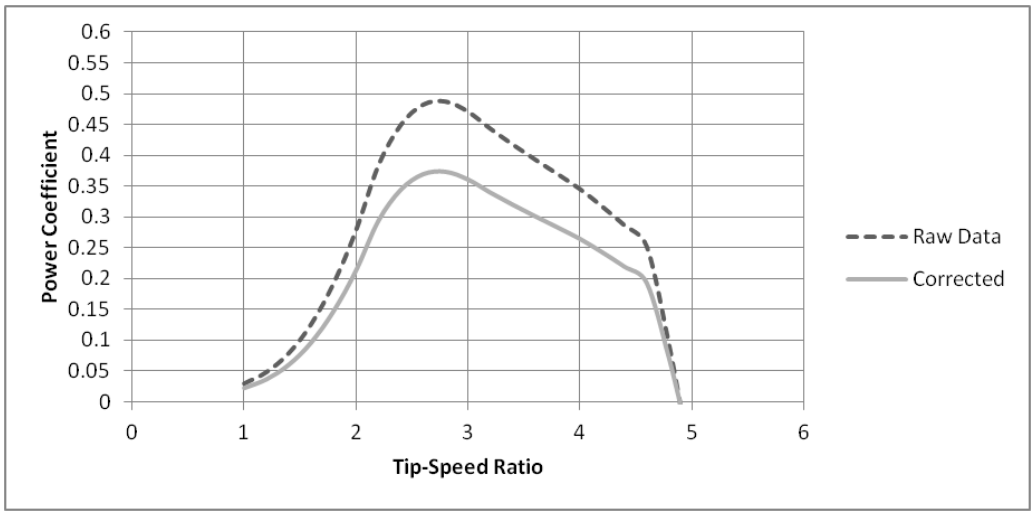

Figure 10: Raw and corrected power coefficient curve

From the power coefficient plot, the best operating point for the turbine was determined to be at a tip-speed ratio of 2.7.

The rotor was then modeled under wind speeds from 2 m/s to 38 m/s (the maximum sustained wind recorded in the target area). The rotational speed of the turbine was allowed to vary to maintain the optimal tip-speed ratio. Output power, rotor torque, and aerodynamic forces on the entire rotor as well as the individual blades were recorded over this range. The rotor was also analysed in a parked condition at a wind speed of 50 m/s to obtain the rotor loads at the IEC 61400-1 Class IA reference state.

While the results show that outputs in the megawatt range are theoretically possible from this turbine, in practice, this will require a larger generator and heavier structure. Given that large power outputs will only occur at high wind speeds that are very rarely recorded, it was deemed beneficial to govern the turbine to 35 RPM and apply a cut-out wind speed of 26 m/s. This greatly reduces aerodynamic loads on the rotor and torque on the driveshaft, allowing these components to be lighter and less costly. While the annual output of the turbine is decreased as a result, the cost of building the turbine structure and components large enough to withstand the increased dynamic forces would cause the system to be prohibitively expensive.

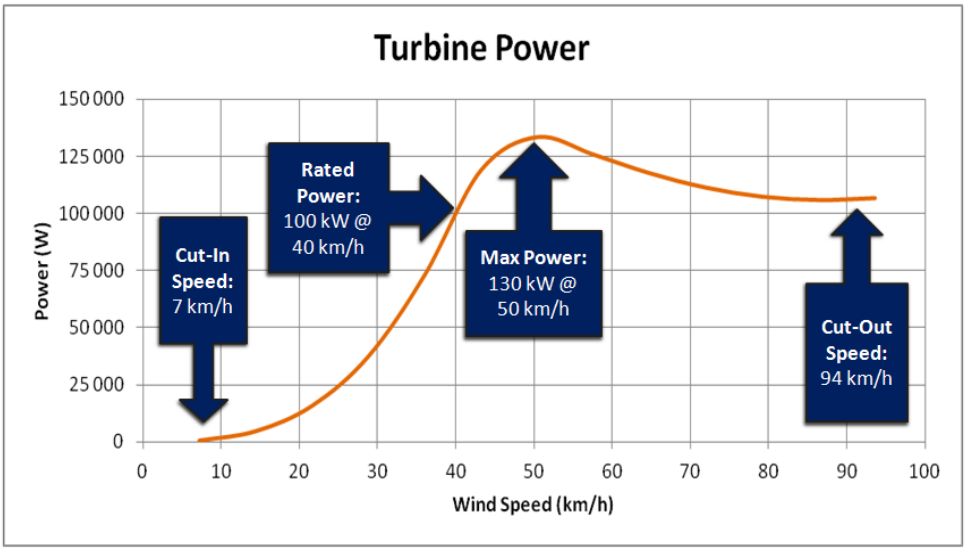

Figure 11: Turbine Power Curve

Estimated required sizes for the shaft and tower are shown below for both the governed and unlimited turbine. Due to the significant increase in component size for the unlimited turbine, it is estimated that the increase in system cost would outweigh the additional power generated. It is expected that governing the turbine will increase financial benefit over the life of the system.

Table 8: Component size estimate for unlimited and governed turbines

Control State	Unlimited	Governed
Required Shaft OD (mm)	800	400
Required Tower OD (mm)	4900	3000
Estimated Annual Output (MWh)	585	375

With the turbine performance specified, a torque curve for the rotor running at the best operating point was generated. This curve corresponds to the desired torque-speed characteristic of the generator.

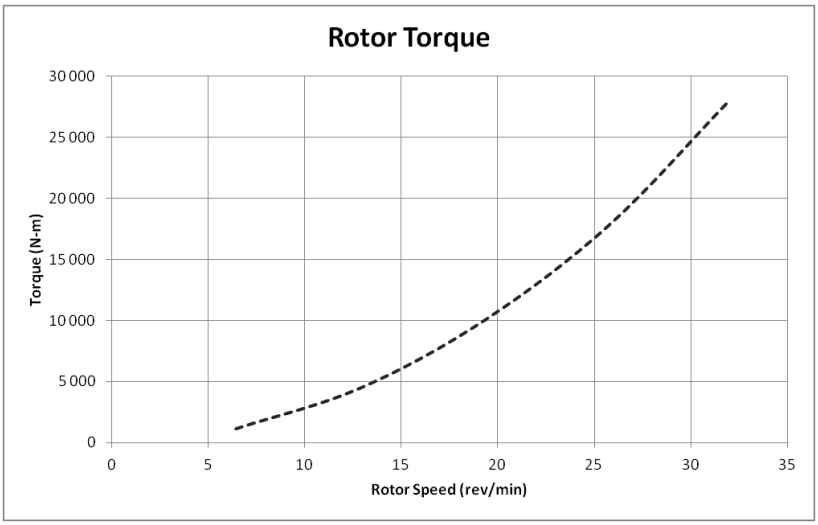

Figure 12: Rotor Torque Curve

6.3 Computational Fluid Dynamics

To help validate the results obtained from QBlade, a simple two-dimensional computational fluid dynamics simulation was carried out using ANSYS CFX. The two-dimensional analysis is not as accurate as a full three-dimensional analysis, but does allow for greatly reduced computational demands.

6.3.1 Mesh Setup

An important part of a CFD analysis is the meshing setup. Since the forces on the turbine blades (namely, lift and drag forces) are driven by boundary-layer effects, the mesh around the blades must be fine enough to accurately capture these effects. The approximate boundary-layer thickness for a laminar flow is given by the following formula: [15]

Equation 4: Boundary-Layer Approximation

$$\partial \sim {}^{4.91x}/_{\sqrt{Re_x}}$$

Where ∂ is the boundary-layer thickness, x is the characteristic dimension (in this case, the position along the chord of the airfoil), and Re_x is the Reynolds number in terms of the characteristic dimension. For turbulent boundary layers, the thickness is given by: [15]

Equation 5: Boundary Layer Approximation

$$\partial \sim {}^{0.382x}\Big/_{Re_x^{1/5}}$$

Assuming that transition from laminar to turbulent flow occurs at a Reynolds number of 50 000, the thickness of the boundary layer on the VAWT blade from the leading edge to the trailing edge was calculated. This is shown in the figure below.

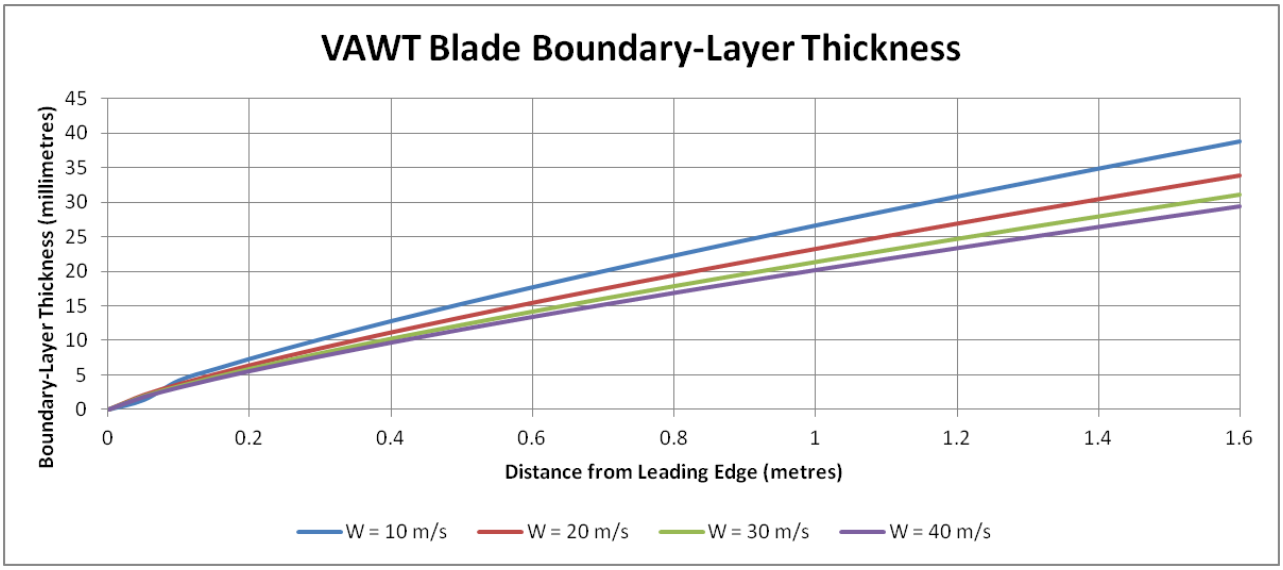

Figure 13: Boundary-layer thickness at various stream speeds

It was found that the boundary layer over the blade will be at least 6 millimetres thick over most of the blade. Therefore, the mesh at the blade surface was fixed to a maximum size of 3 millimetres and allowed to inflate at a fixed rate at increased distances from the surface. This allows for resolution of the boundary layer while allowing for larger element sizes at less critical locations, reducing required simulation time.

The element size of 3 millimetres was arrived at by conducting a mesh refinement study. The same simulation was run multiple times with progressively finer mesh, until the results ceased to vary with decreased element size. In this way, discretization errors in the simulation were eliminated.

6.3.2 Domain and Interface Setup

The simulation was divided into three domains, as shown in the figure below. The far field and the centre near-field (shown in blue) use a stationary frame of reference, while the annular near field (shown in red) uses a frame of reference that rotates clockwise at a constant speed equal to the operating speed of the turbine. The mesh and wall boundaries that define the blades are allowed to rotate with the frame of reference. In this way, the motion of the blades is simulated.

ANSYS CFX allows a number of schemes for modelling the interface between the rotary and stationary domains. These are:

- Frozen rotor
- Stage
- Transient rotor-stator

The frozen-rotor approach assumes a quasi-steady-state (i.e. stationary) rotor, and simply adds the centrifugal and Coriolis components of the fluid velocity in the rotating domain. The stage approach also assumes a quasi-steady-state rotor, but achieves increased accuracy by averaging the flow variables circumferentially around the interface. The transient rotor-stator approach solves the simulation using the rotating domain without using any simplifications. Because of the small number of blades, the aerodynamic effects on the VAWT vary significantly depending on blade azimuth angle; for this reason, the transient rotor-stator approach was required to achieve an accurate result. [16]

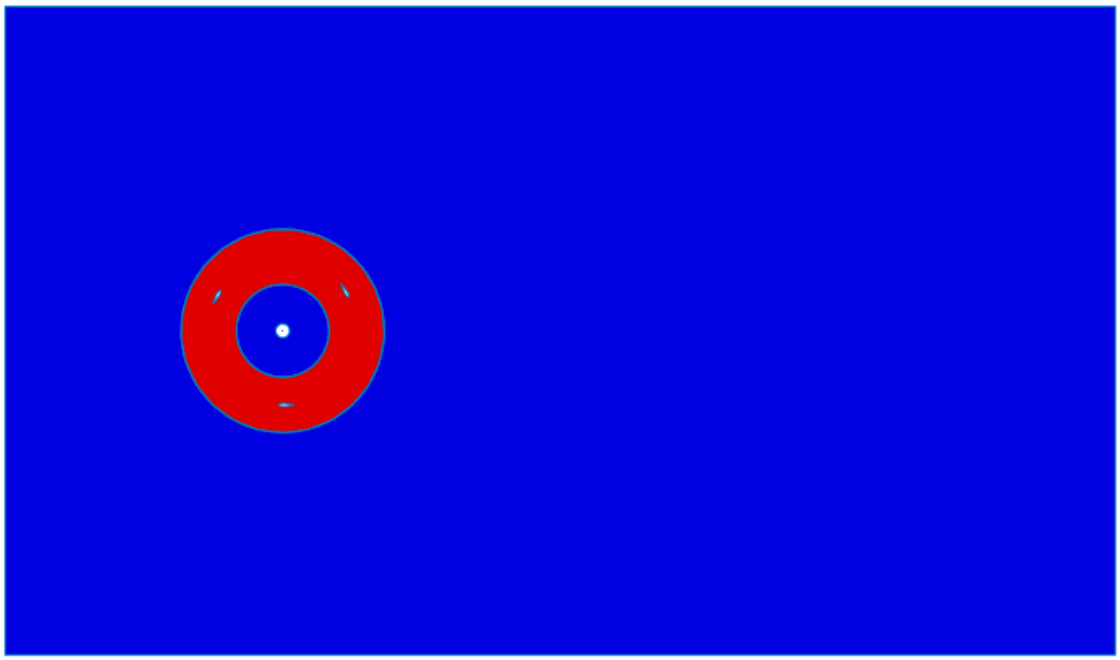

Figure 14: CFD analysis domain setup.

6.3.3 Boundary Conditions

To simulate an incoming wind velocity, an inlet boundary condition was placed at the upstream end of the stationary domain. This inlet was assigned a constant velocity. The opposite end of the stationary domain was assigned as an outlet, allowing flow to exit against atmospheric pressure. The simulation was refined to ensure that the outlet was sufficiently far downstream for the fluid wake to stabilize prior to exiting the simulation. The sides of the stationary domain were given a free-slip wall condition. This allows the fluid to move freely parallel to the wall, but requires that the velocity normal to the boundary be zero. This allows the simulation to be bounded without the added complexity of an outlet boundary condition. However, care must be taken to ensure the disturbance of the turbine on the flow does cause non-zero normal velocity near the boundary; otherwise the width of the far-field domain must be increased.

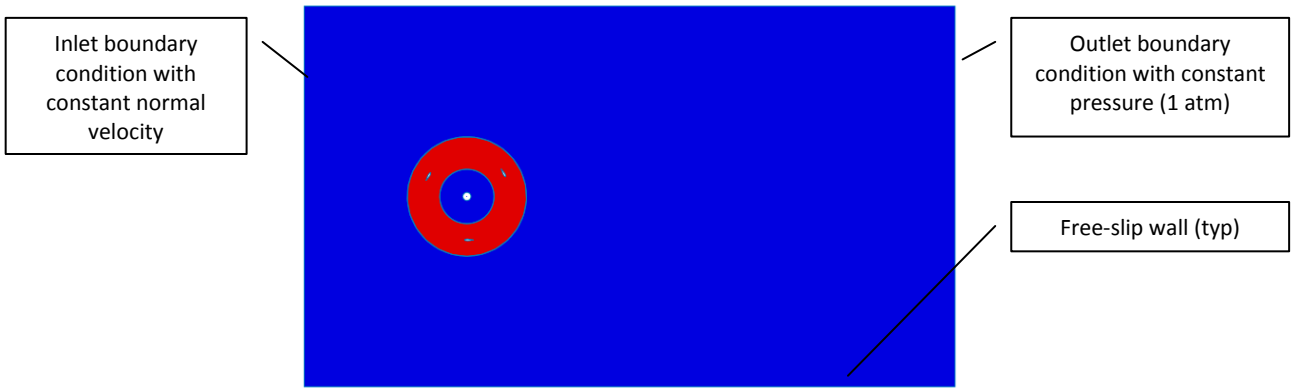

Figure 15: Outer boundary conditions

To simulate the blades and tower, a no-slip smooth wall condition was assigned to the edges of the rotary domain corresponding to the blades and the edges of the central stationary domain corresponding to the tower. Future simulations may use a rough wall condition at these edges to simulate the effects of surface damage or icing on the performance of the turbine.

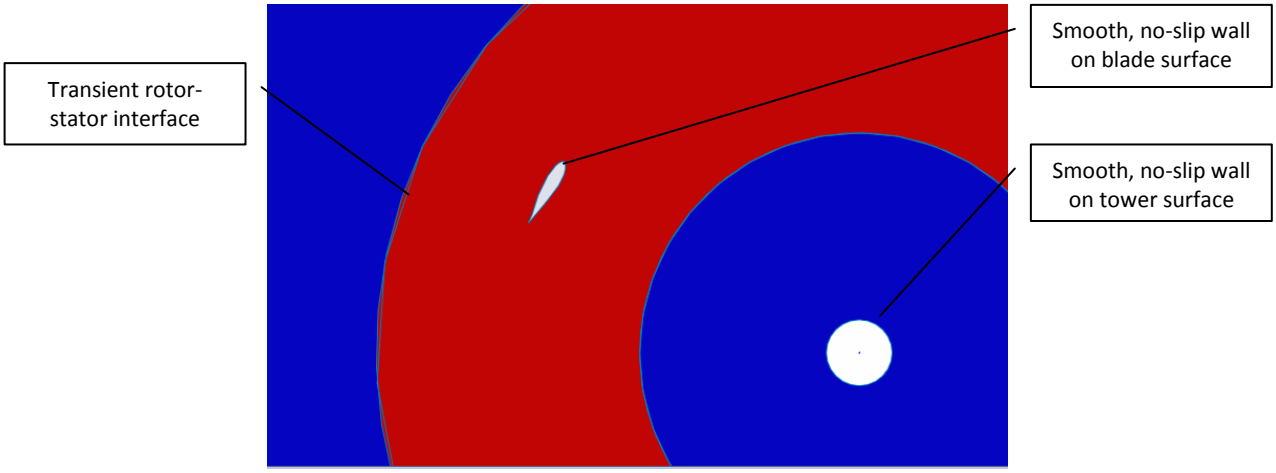

Figure 16: Detail of blade and tower boundary conditions

Because of the two-dimensional nature of the simulation, a symmetry boundary condition was applied to the upper and lower surfaces of all domains. This effectively assumes that no three-dimensional flow will take place in the model.

6.3.4 Solver Setup and Results

The solver was run for approximately 3 turbine revolutions, or 5 seconds at 35 revolutions per minute. This allowed sufficient time for the turbine to reach steady state from the initial conditions. All domains were given an initial velocity equal to that of the inlet. The simulation took approximately 8 hours to run.

As expected, the results of the CFD simulation show a somewhat higher average power output than that predicted by QBlade. This is primarily because the 2D simulation does not account for three-dimensional flow effects such as blade tip losses. Tip loss is an effect that causes reduced lift and increased drag near the extremities of an airfoil because of the high-pressure air on the lower foil surface 'spilling over' to the low-pressure zone on the upper surface.

The torque and power computed for the turbine from the simulation at 10 m/s wind speed and 35 revolutions per minute are shown below. The first few seconds of data vary significantly because of the simple initial conditions; however, by the end of the simulation the torque has stabilized somewhat. Future work for this project would include running the simulation for longer to ensure that the output has fully reached steady-state. A second simulation was run at 8 m/s wind speed and 28 revolutions per minute. This simulation was initialized using the final result of the first simulation to give more accurate initial conditions. This can be seen in the reduced torque fluctuation at the beginning of the output data.

It should be noted that the data in the plots below is not the raw output from the simulation. Because the simulation is in two dimensions, the raw data is in terms of torque per unit length. To obtain the results below, the raw output was multiplied by the blade length of 20 metres. Power was calculated using the definition of rotary power:

Equation 6: Rotary Power Equation

$$P = T\omega$$

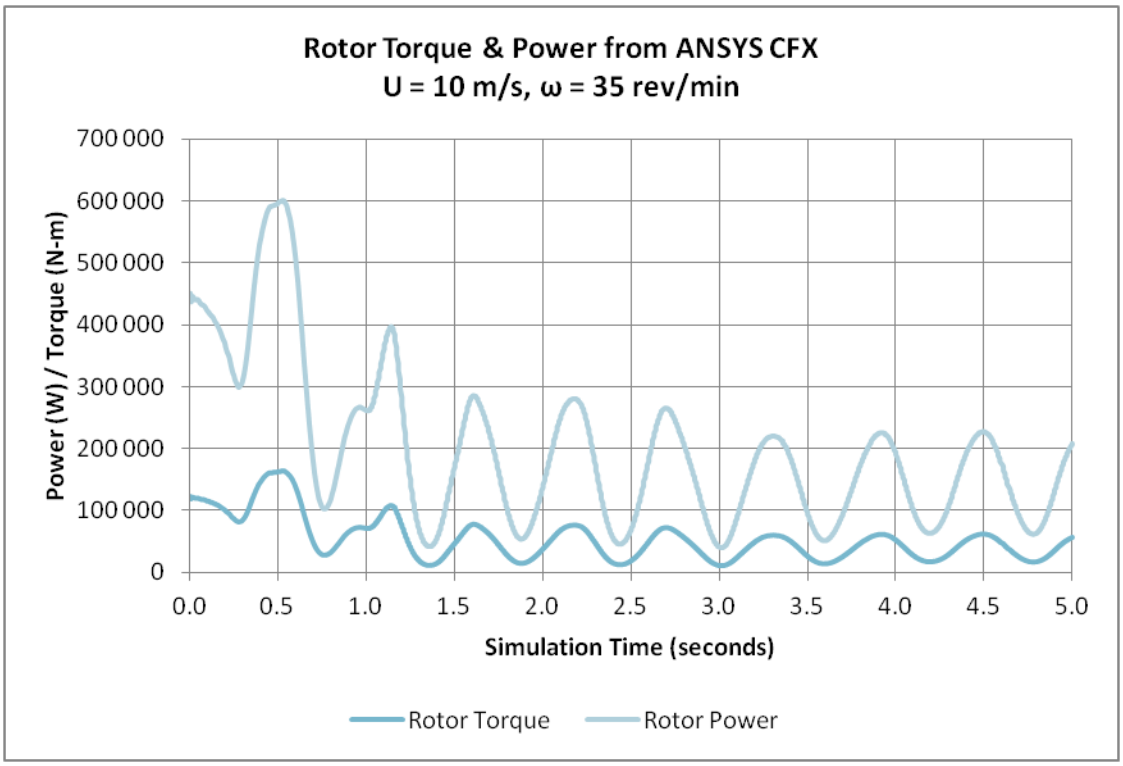

Figure 17: Results of CFX simulation, 10 m/s wind speed

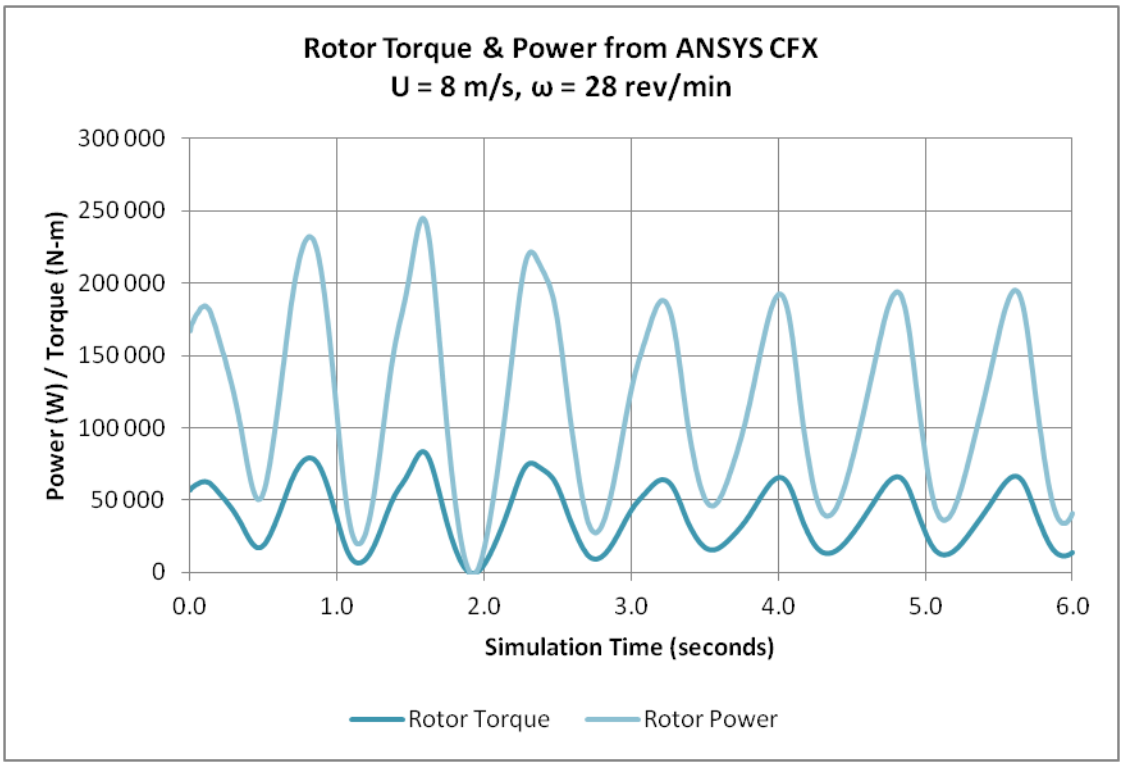

Figure 18: Results of CFX simulation, 8 m/s wind speed

At a wind speed of 10 metres per second and a rotational speed of 35 revolutions per minute, the average power output was approximately 140 kW. Applying a 96% efficiency to account for generator losses, the output becomes 134 kW. At 8 metres per second and 28 revolutions per minute, the average power is 98.5 kW, or 94.6 kW with the generator efficiency applied. A comparison of these results with the results predicted from QBlade is shown in the table below.

Table 9: Comparison of power output calculated by QBlade and ANSYS CFX with and without tip loss correction

Case	Wind Speed (m/s)	Rotor Speed (rev/min)	Power from CFX, No Tip Loss (kW)	Power from QBlade With Tip Loss Correction (kW)	Power from QBlade Without Tip Loss Correction (kW)
#1	10	35	140	96	120
#2	8	28	98.5	47	58

For Case #1, the performance of the turbine (not accounting for tip loss) is similarly predicted by QBlade and CFX. However, for the lower-speed case, the power predicted by QBlade is significantly lower than that predicted by CFX. Further refinement of the CFD model is needed to verify whether the power output predicted by the flow simulation is accurate; however, computational limitations prevented this from being accomplished during the time allotted for the project.

6.3.5 Future CFD Modelling

Further work to be carried out on the project would include a full three-dimensional CFD model of the turbine. This would include the tower, rotor, struts, and strut fairings. In place of the symmetry boundary conditions on the top and bottom faces of the domain, the top plane would be assigned a free-slip wall condition (similar to the sides of the 2D simulation) and the bottom plane would be assigned a no-slip wall condition to simulate the ground. The domain setup and interface would be similar to that of the 2D simulation.

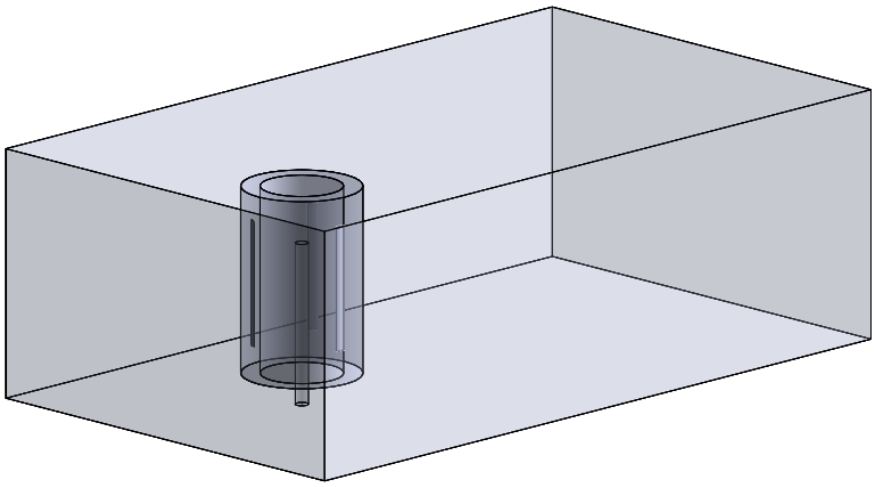

Figure 19: Domain setup for 3D simulation. Struts are not shown.

While the setup for the 3D simulation was carried out, computational limitations prevented it from being solved. Research shows that significant computing power and approximately 40 hours of computational time per single turbine revolution is required to obtain accurate results with a full 3D simulation (Mukinovic, M; Brenner, G; Rahimi, A; *Aerodynamic Study of Vertical Axis Wind Turbines,* Clausthal University of Technology).

6.4 Dynamic Modeling

Since Newfoundland and Labrador is known for having unpredictable wind conditions; one of the project goals was to verify operation of the turbine design in variable wind conditions. In order to do this a simple bond graph model was created using 20-sim modeling/simulation software. Bond Graphs are a graphical representation of a dynamic system utilizing a bi-directional flow of energy in the system. They are similar to and can be combined with block diagrams. [17]

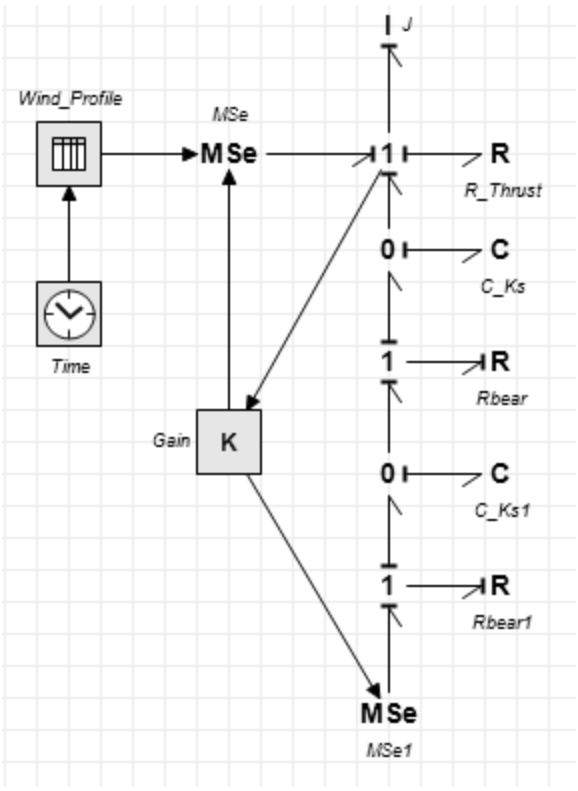

Figure 20: Simple wind turbine Bond graph

Input for the model comes from a data table comprised of values for wind speed at set times. The 20-sim software uses linear interpolation for points between the values in the table. [18] The motion of the model is derived from the two modulated effort sources in terms of torque. The Q-blade data generated was curve fit using a two variable approach to derive the following torque equation in terms of a wind speed in m/s and current rotational velocity of the turbine in RPM that is implemented in MSe.

Equation 7: Wind Torque Curve Fit

$$Twind = (A1 * V^8 + B1 * V^7 + C1 * V^6 + D1 * V^5 + E1 * V^4 + F1 * V^3 + G1 * V^2 + H1 * V + I1) * RPM^3 + (A2 * V\text{^}8 + B2 * V\text{^}7 + C2 * V\text{^}6 + D2 * V\text{^}5 + E2 * V\text{^}4 + F2 * V\text{^}3 + G2 * V\text{^}2 + H2 * V + I2) * RPM\text{^}2 + (A3 * V\text{^}8 + B3 * V\text{^}7 + C3 * V\text{^}6 + D3 * V\text{^}5 + E3 * V\text{^}4 + F3 * V\text{^}3 + G3 * V\text{^}2 + H3 * V + I3) * RPM + (A4 * V\text{^}8 + B4 * V\text{^}7 + C4 * V\text{^}6 + D4 * V\text{^}5 + E4 * V\text{^}4 + F4 * V\text{^}3 + G4 * V\text{^}2 + H4 * V + I4)$$

MSe1 utilizes a torque equation derived from the desired generator curve and is solely in terms of RPM.

Equation 8: Generator Torque Curve Fit

$$Tgen = 0.95793146 * RPM\text{^}3 - 13.479623 * RPM\text{^}2 + 394.351217 * RPM - 355.79315$$

The model also factors in the inertia of the complete turbine assembly, the compliance in the drive shafts and friction in the supporting bearings. The constants utilized in the preceding equations and model can be found in Appendix B.

The wind profile, as seen below, used to simulate variable wind speed was derived from the extreme operating gust model for a class IA turbine laid out in the IEC 61400-1 standards. The gust profile was calculated using Vhub = 10m/s, z = 24m and D = 16m. Relevant excerpts from the standards are found in Appendix C. This profile was repeated over a period of 500s and results for turbine rotational velocity were obtained.

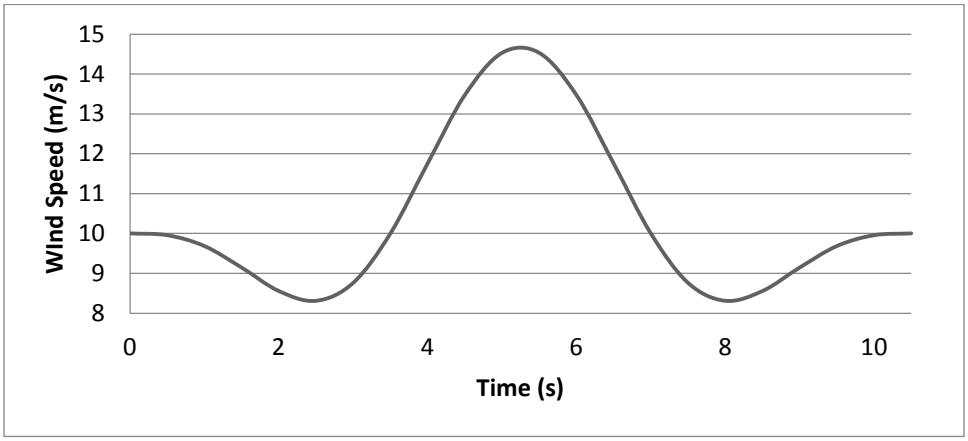

Figure 21: Wind Speed Profile

As seen in the figure below, the gusting wind created a very small ripple in the rpm over the course of the run as the turbine reached a steady state value. The difference between local maximum and minimum was only 0.047 RPM.

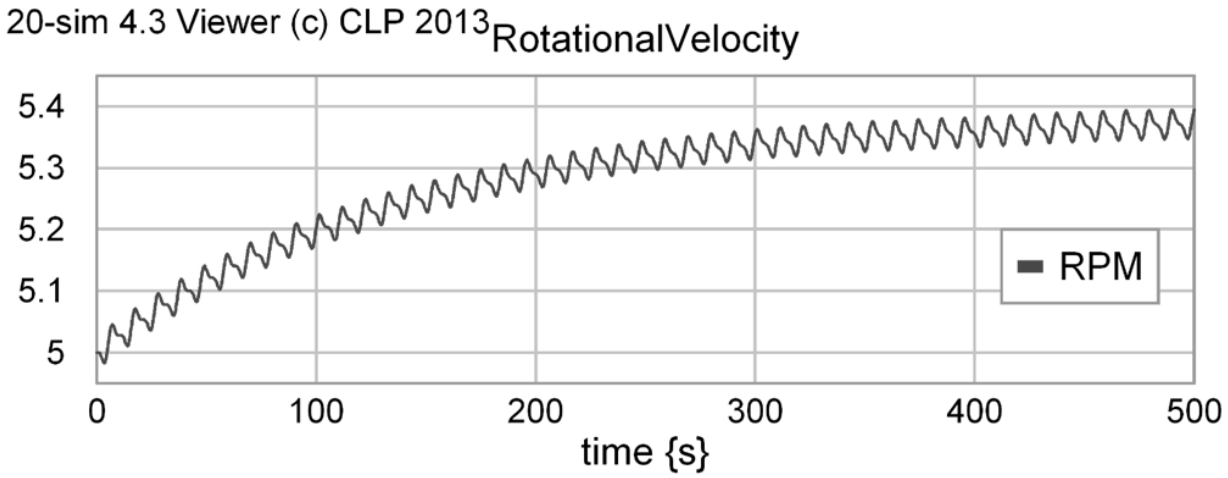

Figure 22: Resulting Turbine RPM

7 Materials Selection

For structural design it is important to consider all materials appropriate to the application. For the design of this turbine, the material should be cost effective and capable of providing the required properties for each application.

For the turbine blades, the material selection was completed using stress analysis, Classical Lamination Theory and Finite Element Analysis based on the required stresses that will be applied by lift, drag and centripetal forces. It was determined that the material should have the following attributes:

- Suitable strength to weight ratio
- Rigid
- Able to withstand calculated shear and normal stresses
- Weather resistant
- Fatigue resistant
- Will not cause galvanic corrosion on struts
- Smooth surface finish for aerodynamic purposes

Materials that were considered were steel, aluminum, and composites. Steel can be immediately rejected due to weight. Aluminum would satisfy the weight requirement, but

exhibits poor fatigue resistance. For this reason, the decision was made to use a composite material. Some types of composites that can be neglected immediately are carbon fibres because they have unsuitable galvanic corrosion properties and higher cost. Through research, it was found that glass-fibre composites are commonly used in modern wind turbines and exhibit favourable mechanical properties. E-glass fibre was determined to be optimal for this application, as described in Section 8.1.1 of this report. The following properties are associated with the laminae orientation utilized:

Table 10: Mechanical properties of E-Glass Fibre [19]

Density	1 900 kg/m^3
Tensile Yield Strength	52 MPa
Modulus of Elasticity	20 GPa
Shear Modulus	2.85 GPa
Poisson's Ratio	0.13

The cylindrical support structure of the turbine will be made of A35 structural steel, a cost-effective material typically used in larger structures. This steel is subject to change upon contacting manufactures. The properties of A35 steel are listed in the table below:

Table 6: Mechanical properties of A35 structural steel [20]

Density	7 800 kg/m^3
Ultimate Tensile Strength	400-550 MPa
Tensile Yield Strength	250 MPa
Modulus of Elasticity	200 GPa
Shear Modulus	79.3 GPa
Coefficient of Thermal Expansion	13.0 (10^{-6} m/m*K)
Poisson's Ratio	0.260

The driveshaft will be manufactured out of AISI 4340 steel. This steel provides the optimal machinability properties and is typically used in many industrial rotational engineering applications, such as large shafts and axles, for its mechanical properties. These properties are listed below:

Table 7: Mechanical properties of AISI 4340 steel [20]

Density	7 850 kg/m^3
Ultimate Tensile Strength	1.11 GPa
Yield Tensile Strength	710 MPa
Modulus of Elasticity	205 GPa
Shear Modulus	80.0 GPa
Coefficient of Thermal Expansion	12.3 (10^{-6} m/m*K)
Poisson's Ratio	0.29

The struts and hub will be manufactured out of AISI 1045 steel. For the struts, this material allows for a relatively small diameter structure compared to structural steels. The smaller the structure the better for the application of a fairing that will reduce the amount of drag forces applied to the strut. For the hub, strength requirements are similar to the struts; AISI 1045 provides excellent strength properties for rotational components. In addition, use of the same material for the struts and hub will help to mitigate galvanic corrosion.

Table 8: Mechanical properties of AISI 1045 Cold Drawn Steel [20]

Density	7 850 kg/m^3
Ultimate Tensile Strength	625 MPa
Yield Tensile Strength	530 MPa
Modulus of Elasticity	205 GPa
Shear Modulus	80.0 GPa
Coefficient of Thermal Expansion	11.5 (10^{-6} m/m*K)
Poisson's Ratio	0.29

8 Structural Design

In addition to operating at peak aerodynamic efficiency it is important to design a VAWT that can withstand lift forces, drag forces and wind loads. Structural analysis was performed on individual components of the VAWT since each part was subjected to different loads. The following components were individually analyzed:

- Blades
- Struts
- Central Hub Column
- Tower

The structural analysis includes solid mechanics, manufacturing constraints, maintenance, and transportation concerns, finite element analysis (FEA) and vibration considerations.

8.1 Blades

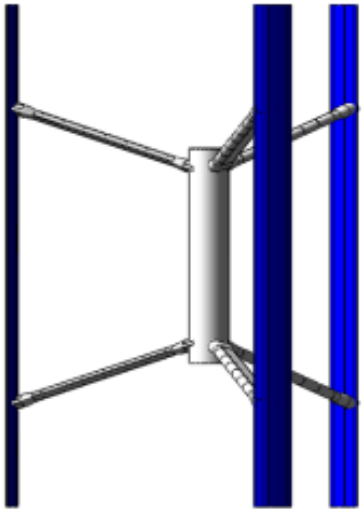

Figure 23 – VAWT Blades

The blade requirements include rigidity, favourable weight to strength ratio, smooth surface finish and to not cause galvanic corrosion on the struts. As such, an E-glass/epoxy composite, more commonly known as fibreglass, was selected as the material for the blades.

8.1.1 Manufacturing Method

The blades will be manufactured by stacking several composite laminae of varying orientations until a desirable thickness is achieved. These hollow blades need to be thick enough to withstand the worst possible aerodynamic and centripetal forces but thin enough to reduce weight and therefore, cost. To determine the optimal dimensions and material, three separate analyses were performed. The first was a solid mechanics analysis, used to calculate the maximum thickness of the turbine blades based on the bending moment due to the maximum aerodynamic and centripetal forces. The second analysis examines the turbine blade as a composite material using Classical Lamination Theory (CLT) to determine the appropriate material/dimensions. The third analysis involved using SolidWorks FEA analysis to validate the dimensions obtained from stress and CLT analyses.

8.1.2 Preliminary Stress Calculations

To model the aerodynamic and centripetal forces loading on the turbine blades to develop a relationship for the optimal strut configuration, the loads were assumed to be uniformly distributed. The straight design of the blade allows for the model to be represented as follows:

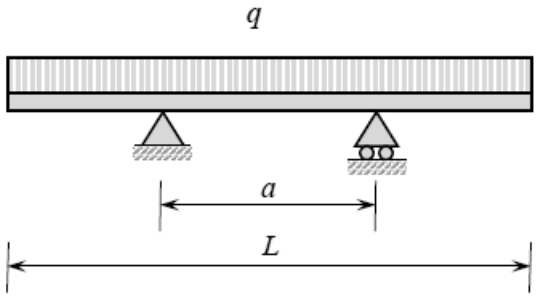

Figure 24: Loading on Turbine Blades

The following relationship was developed to determine the optimal strut spacing based on the length of the blade. [21]

$$a/L = 0.586$$

Where *a* is the spacing between the struts and L is the length or height of the blade. Therefore, the optimal strut spacing is 58.5% of the turbine blade length. Calculations are shown in Appendix D.

In the case of a VAWT blade, the maximum bending stresses, caused by aerodynamic and centripetal forces, will develop at the center of the beam. There is also a smaller torsional effect caused by an aerodynamic moment acting along the length of the blade. In order to determine the proper composite material for the turbine blades, bending and torsional analysis had to be performed to obtain the required thickness of the hollow rectangular support structure. For the solid mechanics and Classical Lamination Theory (CLT) analyses, it was assumed that this support structure takes 100% of the stresses caused by aerodynamic and centripetal forces. The DU 06-W-200 airfoil shape will be developed through the use of fairings, which will be assumed to take 0% of the load. Therefore, the rectangular support structure was analyzed.

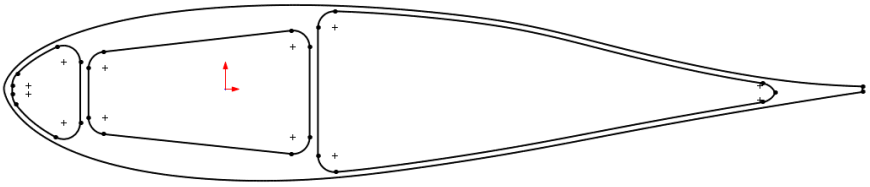

Figure 25 – Cross-Sectional View of Blade

The forces on the blade will include aerodynamic lift and drag, as well as centripetal loads induced from the rotor speed. These forces were obtained from the aerodynamic analysis and resolved into components in the x and y directions (longitudinal and transverse) of the blade profile. It was found that transverse centrifugal and aerodynamic forces were predominant.

Figure 26: Blade forces from aerodynamic analysis and centripetal force calculations

Since the bending stress will dominate the design, it would be beneficial for the stresses to act along the glass fibres, not perpendicular to them. As such, the majority of the laminae should be in the 0 degree orientation. The percentage of lamina orientations is as follows:

0 degrees – 60%

90 degrees – 10%

+-45 degrees – 30%

Based on these orientations, tables 5.11 and 5.13 from the course notes for ENGI 8982: Mechanical Behaviour of Composites were used to obtain the failure criteria assuming a factor of safety of 2:

$$\sigma_{ft} = 104\ MPa/FOS = 52\ MPa$$

$$\sigma_{fc} = 314\ MPa/FOS = 157\ MPa$$

$$\tau_f = 54\ MPa/FOS = 27\ MPa$$

To determine the thickness required to resist the bending stresses, the bending formula was used:

Equation 9: Bending Stress

$$\sigma = \frac{Mz}{I_{zz}}$$

Equation 10: Blade Moment Equation

$$M_{mid} = M_{max} = \frac{q}{4}L^2\left(\frac{a}{L} - \frac{1}{2}\right)$$

q = max aerodynamic and centripetal forces per unit length

$$q = \frac{510710.0168\ N}{20\ m} = 25535.50084\ N/m$$

$$M_{max} = \frac{25535.50084}{4}20^2\left(0.586 - \frac{1}{2}\right)$$

$$M_{max} = 219605.3\ N \cdot m$$

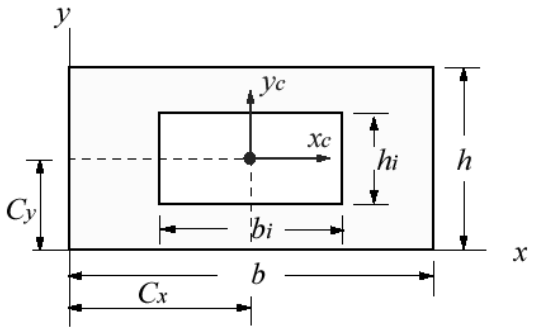

Figure 27 – Moment of Area for a Rectangular Cross-Section[1]

[1] *http://www.efunda.com/math/areas/rectanglehollow.cfm*

Equation 11: Second Area Moment of Inertia

$$I_{zz} = I_{xc} = (1/12)(bh^3 - b_i h_i^3)$$

$$The\ outside\ height\ h\ is\ constrained\ to\ 25\ cm\ \therefore z = 12.5\ cm$$

$$Solving\ for\ I_{zz}\ using\ the\ allowable\ tensile\ axial\ strength\ gives:$$

$$52 \times 10^6\ Pa = \frac{(219605.3\ N \cdot m)(0.125\ m)}{I_{zz}}$$

$$I_{zz} \geq 5.279 \times 10^{-4}\ m^4$$

This allows for a moderate variety of dimensions for b, h_i and b_i. It was important to reduce the amount of material, and number of laminae required, while maintaining the necessary thickness.

8.1.3 Classical Lamination Theory

CLT is used to determine the types of elastic coupling occurring within the structure and the stresses to compare to the allowable stresses. Comparing these stresses will determine whether or not the laminae and material composition will work for the application. To complete this process, the first step is to determine the stiffness matrix or Q matrix.

Equation 12: Stiffness Equations for Q Matrix

$$Q_{11} = \frac{E_{11}}{(1 - v_{12}v_{21})}$$

$$Q_{12} = \frac{E_{11}v_{21}}{(1 - v_{12}v_{21})}$$

$$Q_{22} = \frac{E_{22}}{(1 - v_{12}v_{21})}$$

$$Q_{66} = G_{12}$$

The following is the calculated Q matrix.

4.611E+10	3.689E+09	0
3.689E+09	1.230E+10	0
0	0	4.500E+09

From this Q matrix, the $\overline{Q}$ matrix for laminae orientation 0^0, $\pm45^0$, and 90^0 were found using the following equations.

Equation 13: Stiffness Equations per Orientation for Qbar Matrix

$$\overline{Q_{11}} = Q_{11}\cos\theta^4 + 2(Q_{12} + 2Q_{66})\sin\theta^2\cos\theta^2 + Q_{22}\sin\theta^4$$

$$\overline{Q_{12}} = Q_{12}(\sin\theta^4 + \cos\theta^4) + (Q_{11} + Q_{22} - 4Q_{66})\sin\theta^2\cos\theta^2$$

$$\overline{Q_{22}} = Q_{11}\sin\theta^4 + 2(Q_{12} + 2Q_{66})\sin\theta^2\cos\theta^2 + Q_{22}\cos\theta^4$$

$$\overline{Q_{16}} = (Q_{11} - Q_{12} - 2Q_{66})\sin\theta\cos\theta^3 + (Q_{11} - Q_{12} + 2Q_{66})\sin\theta^3\cos\theta$$

$$\overline{Q_{26}} = (Q_{11} - Q_{12} - 2Q_{66})\sin\theta^3\cos\theta + (Q_{11} - Q_{12} + 2Q_{66})\sin\theta\cos\theta^3$$

$$\overline{Q_{66}} = (Q_{11} + Q_{12} - 2Q_{12} - 2Q_{66})\sin\theta^2\cos\theta^2 + Q_{66}(\sin\theta^4 + \cos\theta^4)$$

$$\overline{Q_0} = \begin{matrix} 46106557377.0492 & 3688524590.16393 & 0 \\ 3688524590.16393 & 12295081967.2131 & 0 \\ 0 & 0 & 4500000000 \end{matrix}$$

$$\overline{Q_{45}} = \begin{matrix} 20944672131.1475 & 11944672131.1475 & 8452868852.45902 \\ 11944672131.1475 & 20944672131.1475 & 8452868852.45902 \\ 8452868852.45902 & 8452868852.45902 & 12756147540.9836 \end{matrix}$$

$$\overline{Q_{-45}} = \begin{matrix} 20944672131.1475 & 11944672131.1475 & 8452868852.45902 \\ 11944672131.1475 & 20944672131.1475 & -8452868852.45902 \\ 8452868852.45902 & -8452868852.45902 & 12756147540.9836 \end{matrix}$$

$$\overline{Q_{90}} = \begin{matrix} 12295081967.2131 & 3688524590.16393 & 0 \\ 3688524590.16393 & 46106557377.0492 & 0 \\ 0 & -8452868852.45902 & 4500000000 \end{matrix}$$

Using the $\overline{Q}$ matrices for 0°, ±45°, and 90°, the A, B and D stiffness matrices can be developed as follows:

Equation 14: Extensional Stiffness Matrix Equation

$$A = \sum_{j=1}^{N} \overline{(Q_{mn})}_j (h_j - h_{j-1})$$

$$A = \begin{matrix} 3.538e9 & 0.6201e9 & 0 \\ 0.6201e9 & 1.841e9 & 0 \\ 0 & 0 & 0.702e9 \end{matrix}$$

Equation 15: Coupling Stiffness Matrix Equation

$$B = \frac{1}{2} \sum_{j=1}^{N} \overline{(Q_{mn})}_j ({h^2}_j - {h^2}_{j-1})$$

$$B = \begin{matrix} 0 & 0 & 0 \\ 0 & 0 & 0 \\ 0 & 0 & 0 \end{matrix}$$

Equation 16: Bending Stiffness Matrix Equation

$$D = \frac{1}{3} \sum_{j=1}^{N} \overline{(Q_{mn})}_j ({h^3}_j - {h^3}_{j-1})$$

$$D = \begin{matrix} 3.920e7 & 0.547e7 & 0.016e7 \\ 0.547e7 & 1.731e7 & 0.016e7 \\ 0.016e7 & 0.016e7 & 0.631e7 \end{matrix}$$

Where A_{16}, A_{26} and the B matrix are equal to zero, there is no Extension-Shear or Bending Extension. However there is Bending Twist due to the non-zero D_{16} and D_{26}.

The stresses found were axial-tension 65.7 MPa, axial-compression -0.423 MPa and shear 4.83 MPa. These values were compared to the maximum allowable stresses and prove that the material is suitable for this application.

8.1.4 Finite Element Analysis

Finite element analysis was conducted to verify the analytical calculations. This was accomplished by modelling the blade cross-section in SolidWorks, fixing the model at the appropriate locations, and applying an evenly-distributed load across the blade surface.

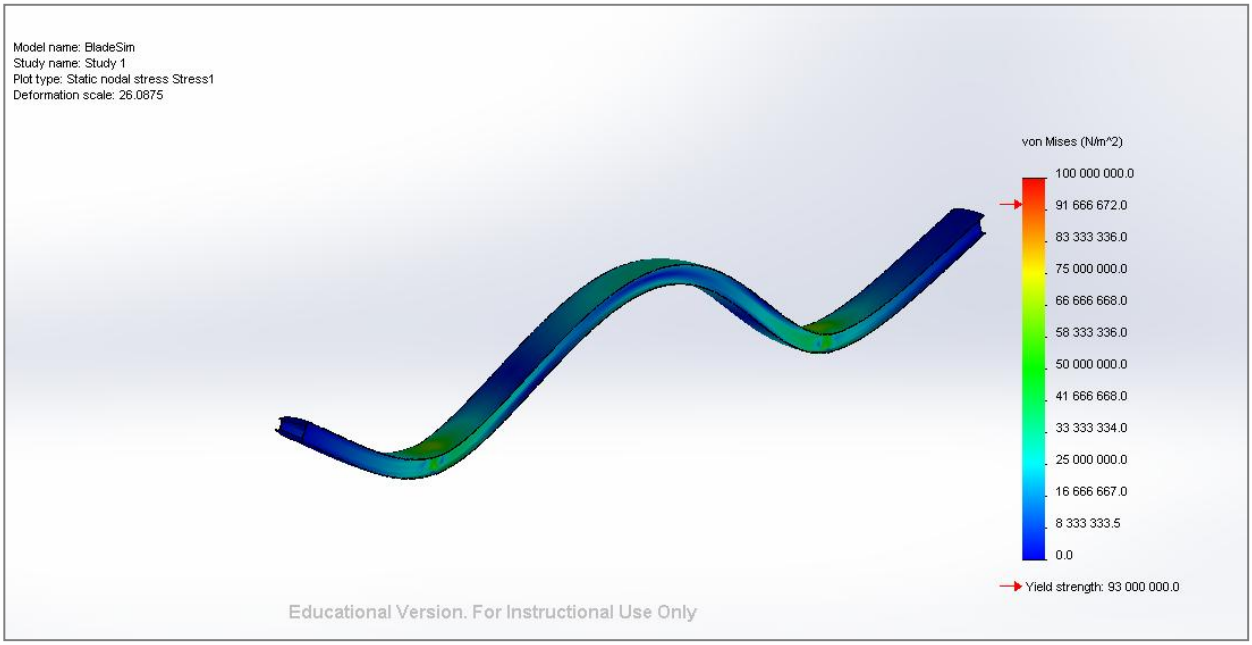

Figure 28 – Finite Element Analysis on Rectangular Cross-Section

The FEA analysis showed that the material should not fail under the worst aerodynamic and centripetal forces under the specified dimensions. From SolidWorks, I_{zz} = 7.000 x 10^{-4} m^4 so the rectangular cross-section should be able to withstand the highest possible loads based on the solid mechanics analysis as well. A wall thickness of 0.05 m was selected, corresponding to 386 E-Glass/epoxy laminae.

8.2 Struts

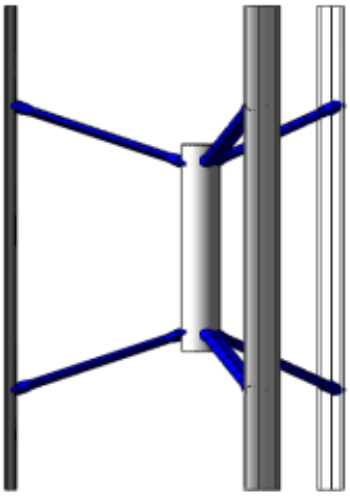

Figure 29 – VAWT Struts

The struts are the structural components connecting the VAWT blades to the support column or hub. The configuration of the strut system was determined by the blade design analysis. The blade was modeled as a simply supported beam, where the support locations represent where the struts are attached. From the blade analysis:

Equation 17: Optimal Support Location

$$a/L = 0.586$$

$$a = 0.586 \times 20\ m = 11.72\ m$$

The optimal strut spacing is equal to the optimal support spacing, calculated to be 11.7 meters apart. The struts were angled in to the hub in order to reduce the moment acting on the central column. To maintain the desired swept area, the strut length at an angle of 18.3^{o} was determined to be 7.6 meters. The optimal cross-sectional shape for the strut is circular due to the axial loading and moments. It was important to minimize weight by using less material and to reduce the outer diameter to minimize drag forces on the struts. With the

inclusion of centripetal and aerodynamic forces, and the weights of the strut and 50% of the blade, bending analysis was preformed.

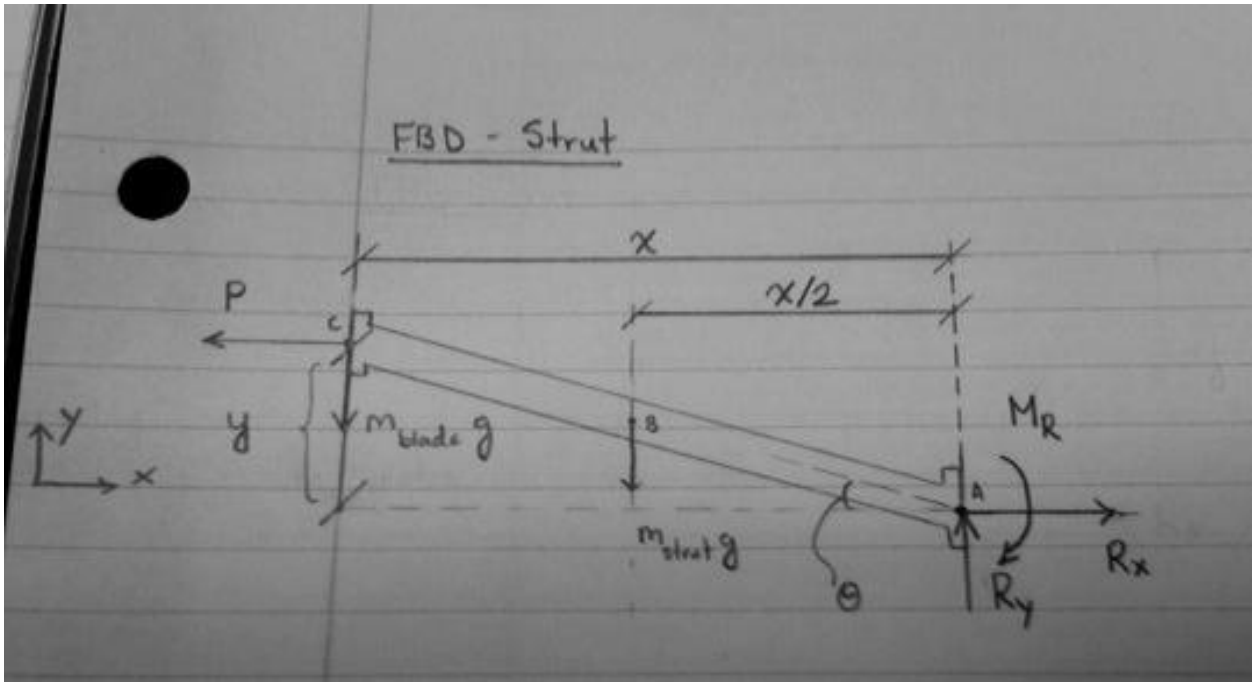

Figure 30 – Free-Body Diagram of Strut

Finding acceptable shaft dimensions was an iterative process since the weight of the strut was dependent on them. Various desired dimensions were substituted into the equation for bending stress using Microsoft Excel. The following calculation uses inner and outer radii values of 0.14 m and 0.18 m, respectively, in Equation 9: Bending Stress.

$$M = \left(\frac{m_{blade}}{2}\right)(g)(x) + (m_{strut})(g)\left(\frac{x}{2}\right) + \left(\frac{P}{2}\right)(y)$$

P = max aerodynamic and centripetal force = 510710.016805733 N

$$M = \left(\frac{4357.4\ \text{kg}}{2}\right)(g)(7.275\ m) + (2403.8\ kg)(g)\left(\frac{7.275\ m}{2}\right) + \left(\frac{510710\ \text{N}}{2}\right)(2.25\ m)$$

$$M = 815814.7231\ N \cdot m$$

$$I = \frac{\pi}{4}({r_o}^4 - {r_i}^4) = \frac{\pi}{4}(0.18^4 - 0.14^4) = 0.000522761\ m^4$$

$$c = r_o = 0.18\ m$$

$$\sigma = \frac{(815814.7231\ N \cdot m)(0.18\ m)}{0.000522761\ m^4} = 2.809 \times 10^8\ Pa$$

The resulting bending stress is less than the tensile yield stress of 625 MPa with a safety factor of 2.22. Therefore, inner and outer diameters of 28 cm and 36 cm, respectively, were selected.

8.3 Central Hub Column

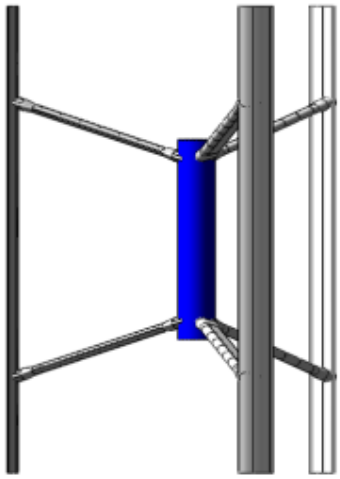

Figure 31 – Central Hub Column

The central hub column of the VAWT is the component that the struts are connected to. It was modelled as a simple vertical cylinder subject to axial stresses from the weight of the

VAWT upper components. Buckling was also considered. The following desired dimensions were used in the analysis:

Outer Diameter: 0.6 m

Inner Diameter: 0.55 m

Length: 8.5 m

Equation 18: Axial Stress

$$\sigma = \frac{F}{A}$$

$$\sigma = \frac{(0.5)(33740\ kg)(9.81\frac{m}{s^2})}{\pi(0.3^2 - 0.275^2)} = 3.66\ MPa \leq 625\ MPa\ (tensile\ strength)$$

Equation 19: Buckling Equation

$$Critical\ Load = P = \frac{n\pi^2 EI}{L^2}$$

n = 4 (both ends fixed)

$$P = \frac{(4)\pi^2(200 \times 10^9\ Pa)(\frac{\pi}{4}(0.3\ m^4 - 0.275\ m^4))}{(8.5\ m)^2}$$

$$P = 204.35\ MN\ (20830826\ kg) \gg 16870\ kg$$

The desired dimensions will not cause the column to fail due to axial stresses or buckling. Therefore, the column will have an outer diameter of 0.6 m, an inner diameter of 0.55 m and a length of 8.5 m.

8.4 Tower

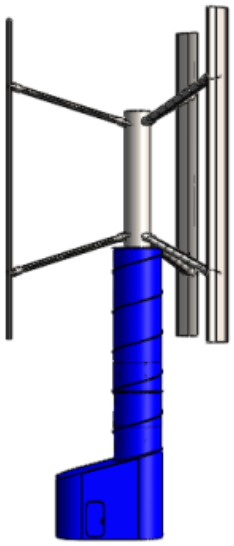

Figure 32 – VAWT Tower

The tower was analyzed as a vertical hollow cylinder subjected to wind loads, rotor forces and the weight of the VAWT itself. This will cause axial stresses, shear stresses and bending stresses in the structure. The tower supports the upper structure and protects the shaft from the elements (wind, rain, snow, etc.). To reduce the amount of material, it was important to minimize the thickness and withstand the worst possible wind loads. To start, 3 meters was selected for the outer diameter with a thickness of 5 centimeters. Bending, axial and shear stress analyses were performed to determine if these dimensions and material are suitable.

The tensile yield strength of A35 structural steel is: [20]

$$\sigma_y = 250\,000\,000\ Pa$$

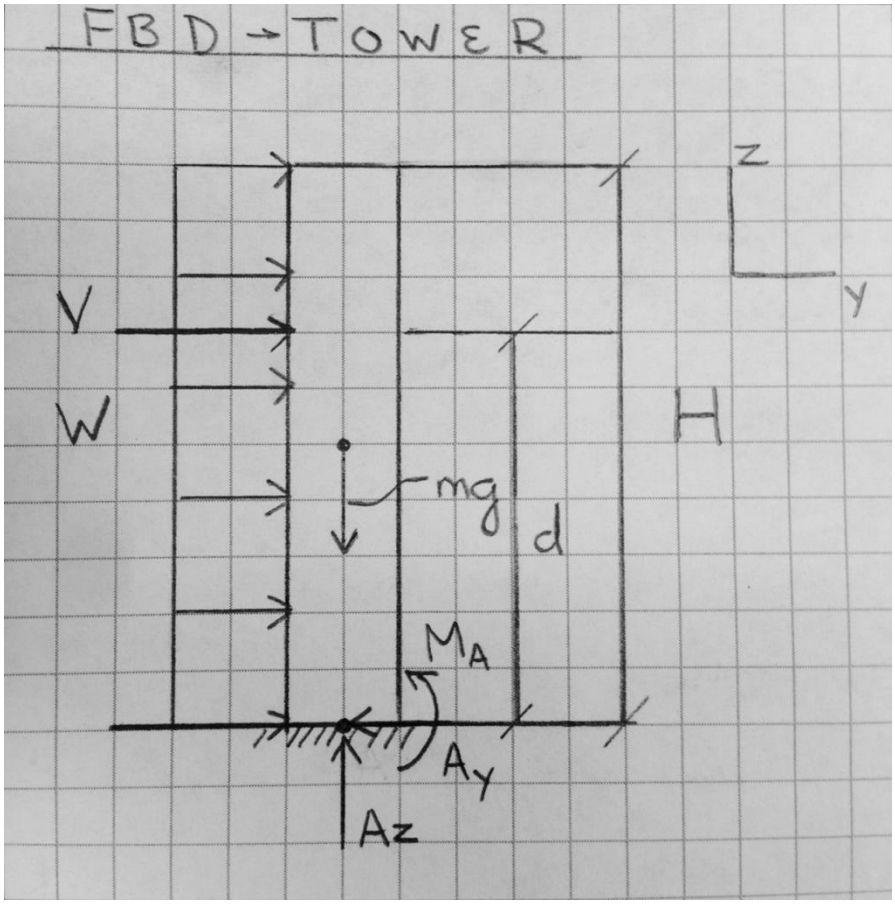

Figure 33 – Free-Body Diagram of Tower

From the figure above,

A_z – reaction force due to axial forces (N)

A_y – reaction force due to shear forces (N)

M_A – reaction moment

W – distributed wind load on tower (N/m)

V – resultant load on tower from wind load on blades (N)

H – tower height (m) = 16 m

d – distance from ground to where V acts (m)

The following values were either selected or known for the structural analysis,

ρ (air density) = 1.25 kg/m^3

v (max wind speed) = 50 m/s

C_D (drag coefficient for a vertical cylinder) = 1.17

H_{total} (height of tower + hub column) = 24.5 m

d (distance from ground to where V acts) = 20.25 m

M_T (mass of the top of the VAWT) = 33 740 kg (estimated)

$M_{Tower} = \pi(ro^2 - ri^2)(H)(\rho) = \pi(1.5^2 - 1.475^2)(16)(7800) = 29{,}160$ kg

8.4.1 Tower – Axial Stress

From basic solid mechanics, the axial stress at the base of the structure is:

$$\sigma_{axial} = \frac{P}{A} = \frac{(29\,160\ kg + 33\,740\ kg)(9.81\frac{m}{s^2})}{\pi(1.5^2 - 1.475^2)} = 2.64\ MPa \ll 250\ MPa$$

Where,

P – axial reaction force (total weight of the VAWT) (N)

A – cross-sectional area of the tower (m^2)

8.4.2 Tower – Shear Stress

The shear stress in the tower structure is caused by wind loads on the tower and the resultant wind loads on the blades (obtained during aerodynamic analysis). The formula for the resultant force caused by wind loading on the tower is:

Equation 20: Resultant Wind Loading

$$F_W = \frac{1}{2}\rho v^2 C_D (D_O H)$$

Where,

ρ – density of air (kg/m³)
v – wind velocity (m/s)
C_D – drag coefficient
*Do*H – projected area where the wind load is applied (for a vertical cylinder, the projected area is the outer diameter multiplied by the height) (m²)*

The following equation was used to convert the single load (F_W) to a distributed load on the tower:

Equation 21: Distributed Load on Tower

$$W = \frac{1}{2}\rho v^2 C_D D_O$$

$$W = 0.5(1.25)(38)^2(1.17)(3) = 3167.8\ N/m$$

Since the wind loading on the blades is constantly varying, the maximum wind force had to be obtained through aerodynamic analysis. Using Excel, the resultant blade wind loads were computed at a variety of azimuth angles (θ). The highest resultant force (F_R) was approximately 60,000 N at an azimuth angle of 32.5 degrees.

From basic solid mechanics, the shear stress at the base of the structure is:

Equation 22: Shear Stress

$$\sigma_{shear} = \frac{V}{A}$$

$$\sigma_{shear} = \frac{(3167.8\frac{N}{m})(24.5\ m)}{\pi(1.5^2 - 1.475^2)} = 332\ kPa \ll 250\ MPa$$

Where,

$V = WH + F_R$

F_R = 114,000 N (resultant max wind load on rotating components (@ 35 RPM))

A – cross-sectional area of the tower (m^2)

8.4.3 Tower – Bending

As with the shear stresses, the bending stresses are caused by wind loads on the tower and the resultant wind loads on the blades.

The tower was modeled as a vertical beam with a fixed support at one end. Therefore, from solid mechanics the maximum bending moment at the base of the structure is:

Equation 23: Bending Moment at Base of Tower

$$M_{max} = \frac{WH^2}{2} + F_R d$$

$$M_{max} = \frac{(3167.8\frac{N}{m})(24.5)^2}{2} + (114{,}000\ N)(20.25\ m) = 3259236\ N * m$$

Where,

W – distributed wind load on the tower (N/m)

H – height of the tower (m)

F_R – resultant blade loading (N)

d – distance from the ground to where F_R acts (m)

The maximum bending moment was then used to calculate the bending stress using the following equation:

$$I = \pi(3^4 - 2.95^4)/64 = 0.2585184074\ m^4$$

$$\sigma_{bending} = \frac{M_{max}(\frac{D_o}{2})}{I}$$

$$\sigma_{bending} = \frac{(3259236\ N*m)(\frac{3\ m}{2})}{0.2585184074\ m^4} = 18.91\ MPa \leq 250\ MPa$$

Where,

M_{max} *– maximum bending moment (N*m)*

$D_o/2$ *– distance from the neutral axis to the point where stress is being calculated (m)*

8.4.4 Tower – Von Mises Stresses

The Von Mises yield criterion was applied to the bending, axial, and shear stresses to determine the Von Mises principal stresses. The maximum Von Mises stress will be used to determine if the selected material or dimensions are valid. If the maximum Von Mises stress is lower than the yield strength of the material, and give an appropriate safety factor, the dimensions and material are valid. Conversely, if the maximum Von Mises stress exceeds the yield strength of the material, then larger dimensions and/or an alternate material are required. The Von Mises stresses were computed in Excel using the following formula:

Equation 24: Von Mises Criterion

$$\sigma_{von-mises} = \left|\frac{(\sigma_{bending} + \sigma_{axial})}{2}\right| + \sqrt{\left[\frac{(\sigma_{bending} + \sigma_{axial})}{2}\right]^2 + [\sigma_{shear}]^2}$$

$$\sigma_{von-mises} = |10.775\ MPa| + \sqrt{[10.775\ MPa]^2 + [0.332\ MPa]^2}$$

$$\sigma_{von-mises} = 21.56\ MPa \leq 250\ MPa$$

8.4.5 Tower – Results

The maximum Von Mises stress was determined to be 21.56 MPa, assuming an inner diameter of 3 meters, a thickness of 5 centimeters and A35 structural steel as the material. The inner diameter should be at least 3 meters to allow for access to the interior components (drive shaft, bearings, etc.) for maintenance purposes. Since the yield strength of A35 steel is 250 MPa, the safety factor of the structure is 11.6. Therefore, the dimensions and material are appropriate for the design.

9 Vibration Analysis

A major consideration with any design with rotating components is vibration. Unwanted vibrations can reduce reliability, performance or even cause failure in structures. To analyze VAWT vibrations, the natural frequency of each component was compared to the operating frequency. The operating frequency was determined by examining how often the aerodynamic and centripetal forces alternate per turbine blade rotation.

Figure 34 – Forces Acting on Turbine Blade Over One Rotation

Where,

Max Force = 510 710 N

Min Force = 413 374 N

Vibrational analysis was performed assuming 40 RPM, the highest possible rotational speed before the breaking system slows the motion. At 40 RPM, the aerodynamic and centripetal forces alternate 3 times / cycle. Therefore the operating frequency is:

$$\omega = \left(40\frac{rev}{\min}\right)\left(2\pi\frac{rad}{rev}\right)\left(\frac{1}{60}\frac{min}{s}\right) = 4.1888\frac{rad}{s}$$

$$\omega\ (in\ hertz) = \frac{4.1888\frac{rad}{s}}{2\pi} = \frac{2}{3} \times 3\ \frac{times}{cycle} = 2\ Hz$$

In addition to the operating frequency, the vortex shedding frequency should also be computed for vortex-induced vibrations. Based on a wind speed of 50 m/s and corresponding Reynolds number of 9077156, the Strouhal number [22] is as follows:

$$Sr = 0.198\left(1 - \frac{19.7}{Re}\right) = 0.198\left(1 - \frac{19.7}{9077156}\right) = 0.1979995703$$

$$Max\ Sr = 0.5\ (use\ this\ value)$$

Equation 25: Strouhal Number

$$Sr = \frac{fL}{U_\infty}$$

Equation 26: Vortex Shedding Frequency

$$f = \frac{SrU_\infty}{D_{tower}} \times \frac{1}{2\pi}$$

$$f = \frac{(0.5)(50\frac{m}{s})}{(3\ m)(2\pi)} = 1.33\ Hz$$

Now the natural frequencies of each component can be calculated and compared to the operating frequency.

9.1 Vibration – Blades

Each blade can be modelled as a simply supported beam to calculate required equivalent mass and stiffness: [23]

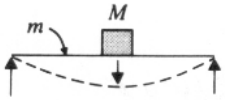

Simply supported beam of mass m carrying a mass M at the middle

$m_{eq} = M + 0.5\ m$

Figure 35 – Equivalent Mass of a Simply Supported Beam

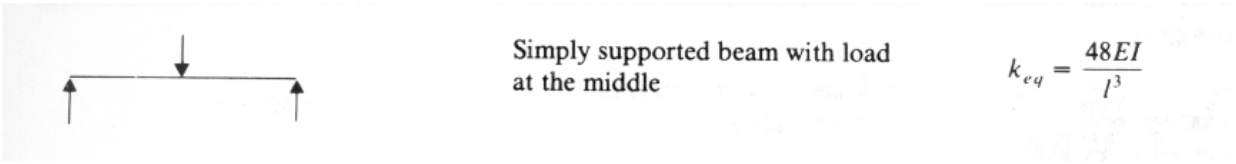

Figure 36 – Equivalent Stiffness of a Simply Supported Beam

$$m_{eq} = M + 0.5m = 0 + 0.5(4355\ kg) = 2177.5\ kg$$

$$k_{eq} = \frac{48EI}{L} = \frac{48(45 \times 10^9\ Pa)(7.02 \times 10^{-4}\ m^4)}{11.7\ m} = 947150\ N/m$$

Equation 27: Natural Frequency

$$\omega_n = \sqrt{\frac{k_{eq}}{m_{eq}}}$$

$$\omega_n = 20.856 \frac{rad}{s} = 3.319\ Hz$$

9.2 Vibration – Struts

Each strut can be modelled as a cantilever beam with an end mass to calculate required equivalent mass and stiffness:

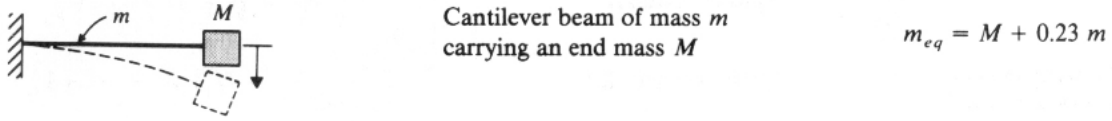

Figure 37 – Equivalent Mass of a Cantilever Beam With an End Mass

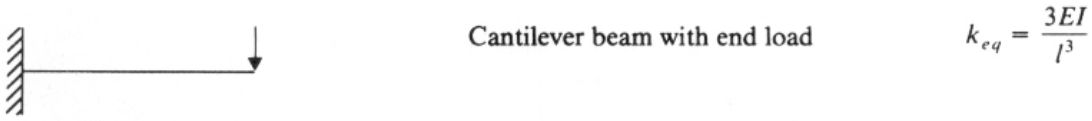

Figure 38 – Equivalent Stiffness of a Cantilever Beam With an End Mass

$$m_{eq} = M + 0.23m = 4357.4 + 0.23(2403.804) = 4910.275\ kg$$

$$k_{eq} = 2 \times \frac{3EI}{l^3} = 2 \times \frac{3(200 \times 10^9)(0.000522761017557341\ m^4)}{7.614993\ m^3} = 1.421\frac{MN}{m}$$

$$\omega_n = 16.3585\frac{rad}{s} = 2.707\ Hz$$

9.3 Vibration – Tower

As with the struts, the tower can be modelled as a as a cantilever beam with an end mass:

$$m_{eq} = M + 0.23m = 33740 + 0.23(29160) = 40447\ kg$$

$$k_{eq} = \frac{3EI}{l^3} = \frac{3(200 \times 10^9)(0.2585184074\ m^4)}{20.25\ m^3} = 18.68\frac{MN}{m}$$

$$\omega_n = 29.49\frac{rad}{s} = 3.42\ Hz$$

9.4 Critical Speed – Drive Shaft

Potential problems in design of drive shafts are critical speeds: where the shaft becomes unstable due to eccentricity or improper balancing, with deflections increasing without upper bound. [24]

Equation 28: Critical Shaft Speed

$$\omega_c = \left(\frac{\pi}{l}\right)^2 \sqrt{\frac{gEI}{A\gamma}}$$

$$\omega_c = \left(\frac{\pi}{7.5}\right)^2 \sqrt{\frac{g(200 \times 10^9)(0.0005541)}{(0.0304024487)(76518)}} = 120\frac{rad}{s} = 1145\ RPM$$

Where,

ω

A = Cross-Sectional Area

γ = Specific Weight = ρg = 76518 kg/m²s²

l = Length Between Bearings/Supports

Since the maximum shaft rotation will be about 40 RPM, the VAWT driveshaft will never be close to the critical shaft speed.

9.5 Vibration – Results

The calculated natural frequencies for each component are tabulated below:

Table 11 – Table of Natural Frequencies and Frequency Ratios

Component	Natural Frequency	Frequency Ratio ω/ω_n
Tower	3.42 Hz	0.58
Struts	2.71 Hz	0.74
Blades	3.32 Hz	0.60
Drive Shaft	1145 RPM (critical speed)	N/A

To check if vibrations will be concerning, the frequency ratios were plotted on the following frequency ratio chart:

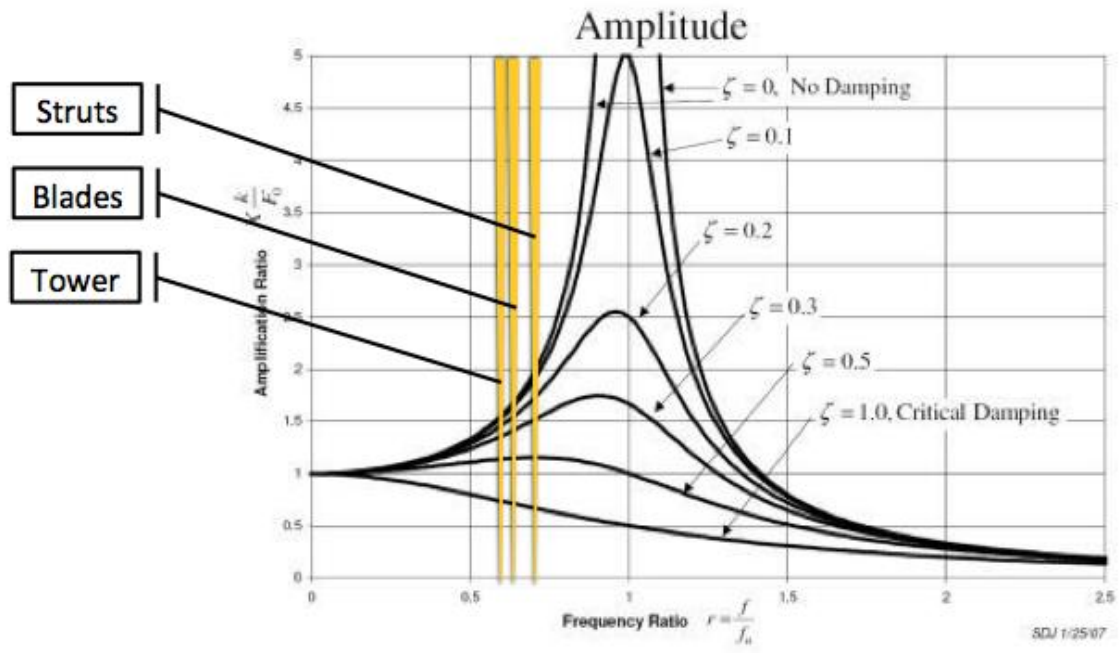

Figure 39: Frequency ratio chart showing position of components[2]

Since all of the maximum frequency ratios for the components are below resonance (where ω and ω_n are equal), the structure should not suffer severe effects from vibration.

10 Mechanical Components

10.1 Initial Driveshaft Design

The design of the turbine driveshaft was initially governed by the torque generated from the rotating blades.

The yield strength of AISI 4340 is:

$$\sigma_y = 420\,507\,000\ Pa$$

[2] *Adapted from http://en.wikipedia.org/wiki/File:Forced_Vibration_Response.png*

Since the maximum principal stress is σ_y and the minimum principal stress is zero, from the Maximum Shear Stress Theory:

$$\tau_{max} = \frac{\sigma_y}{2} = 210\ 253\ 500\ Pa$$

The torsion formula for a solid cylindrical shaft is:

Equation 29: Torsion Formula

$$\tau_{max} = \frac{TDo}{2J}$$

Where,

Equation 30: Polar Moment of Inertia

$$J = \frac{\pi}{2}\left[(\frac{D_o}{2})^4 - (\frac{D_i}{2})^4\right]$$

*T – torque (N*m)*

Do – outer diameter (m)

Di – inner diameter (m)

Using the torsion formula, a multitude of values could be selected for the inner and outer diameters of the shaft provided the calculated torsion does not exceed the allowable shear stress. For the initial sizing, inner and outer diameters of 0.26 m and 0.3 m were selected. From the initial aerodynamic analysis using QBlade, the maximum torque on the drive shaft was approximately 100 000 N*m. Thus, using the torsion formula:

$$\tau_{max} = 43\ 279\ 988\ Pa$$

Since the torsion is less than the allowable shear stress, the selected shaft dimensions are appropriate with a safety factor of 4.9.

10.2 Final Driveshaft Design

To verify that the initially calculated dimensions were suitable for the VAWT, an additional fatigue calculation was performed. This fatigue analysis proved the initial drive shaft to be unsuitable and therefore was recalculated using fatigue criteria and verified using the previous stress calculation. The fatigue analysis procedure utilized correction factors for surface, size, load, temperature, and reliability. The safety factor deemed acceptable was

1.15, this may seem low however the analysis is very conservative by using the worse possible case over an unrealistic sustained period of time. The following equation was used to determine whether or not it has infinite life.

Equation 31: Fatigue Safety Factor

$$FOS_{Fatigue} = \frac{1}{\left(\frac{\sigma_{Alternating}}{Nom.\,Endurance\ Lim.* K_{factors}}\right) + \left(\frac{\sigma_{Mean}}{Ulti.\,Strength}\right)}$$

10.3 Driveshaft – Results

The optimal driveshaft that will produce an infinite life space, will also produce a yielding factor of safety of 4.15. The dimensions were determined to be an outer diameter of 406.4mm and an inner diameter of 355.6mm.

10.4 Driveshaft Components

There are many types of bearings and couplings to consider when designing a vertical rotational shaft. The VAWT, as noted in the previous section, will contain a driveshaft that consists of two equal length shafts. To support and connect these shafts, the bearings and couplings must be able to satisfy the torsional and axial loads. Other design criteria for bearing and coupling selection are life span, reliability, cost and material.

10.4.1 Bearings

When choosing a bearing, it is important to know what types of bearings are available on the market and how functions are required of the bearing. Types of bearings include ball bearings, roller bearings, and thrust bearings. Typically, bearings are manufactured to withstand radial loads, thrust loads, or a combination of both. For the driveshaft of the vertical axis wind turbine, a combination of radial and thrust loading will be required. This led to a comparison of tapered roller bearings and angular contact ball bearings. Angular contact ball bearings are generally used for high rotational speed and relatively lower loads, in contrast to tapered roller bearings which are used for lower rotational speed and

higher loads. With the requirements of a heavy force load at a low rotational speed of approximately 30 rpm, it was decided that the optimal bearing would be a tapered roller bearing.

To determine the required size of the bearing, MUN VAWT Design investigated various bearing manufactures to determine what was available. The bore of the bearing is constrained by the driveshaft outer diameter. MUN VAWT Design checked various bearings and found the best to have the following specifications.

Table 12: Bearing specifications[3]

Manufacturer Identification	**Height (mm)**	**Bore (mm)**	**OD (mm)**	**Mass (kg)**
802086	381	406.4	546.1	183
Dynamic Load Rating (kN)	**Static Load Rating (kN)**	**e**	**Equivalent Load Rating Cr90 (kN)**	**Equivalent Load Rating Ca90 (kN)**
6950	15000	0.43	1760	365

To meet the standards found for wind turbines in Canada, the bearings life span must be greater than 20 years. It was determined that this bearing, under the max loading under the design configuration of having 2 bearings per driveshaft section, will survive longer than 20 years. The following calculation was used to provide this result:

Equation 32: Bearing Life Span

$$Life\ Span = \left[\frac{C}{P}\right]^{a};$$

Where C is the Dynamic Load Rating, P is the applied load and a is 10/3 for roller bearings.

[3] *Bearing specifications courtesy of Schaeffler Technologies GmbH & Co. KG*

10.4.2 Mechanical Couplings

The VAWT drive shaft is required to be sectioned in order to meet the shipping criteria set in the project objectives. A mechanical connection is required to join the sectional drive shaft upon installation and compensate for misalignment and thermal expansion in service. To select a coupling, the features required of the coupling must first be determined. Mechanical shaft couplings can be either rigid, flexible/compensating, or clutch type couplings. For the VAWT driveshaft assembly, the coupling must connect two shafts together, transmit a relatively high torque at low rotational speeds, require minimal maintenance, and provide sufficient flexure and axial relief. Due to the constraints, clutch type and rigid couplings can be eliminated immediately from the design, making the coupling of choice flexible or compensating. With the constraints determined to be minimal maintenance, low cost, and high life expectancy, companies that supply various types of couplings were investigated. These companies include:

- Love-Joy
- Ruland
- Hayes
- Renold

Renold has been contacted regarding information on the "Renold Hi-Tec RB" mechanical coupling that specifies shaft to shaft connection for applications such as wind turbines. The features listed for the coupling include the following:

- Intrinsically failsafe
- Control of resonant torsional vibration
- Maintenance free
- Severe shock load protection
- Misalignment capability
- Zero backlash
- Low cost

The driving features of this coupling are the misalignment capability and maintenance free attributes. These features provide significant advantages over common connections such as constant-velocity joints or universal joints, because they do not require any lubrication and can allow for axial, radial and angular misalignment.

10.5 Generator

In order to eliminate the need for a speed-increasing gearbox between the rotor and generator, it was decided to use a permanent-magnet generator to convert the mechanical power of the turbine rotor to electrical power. Permanent-magnet machines can generate power from zero speed up to their rated speed, which can be as low as 12 revolutions per minute. While these types of generator are generally more expensive than the asynchronous induction machines that have been predominant in the past, they allow for increased reliability and reduced capital cost resulting from the elimination of the gearbox. [25] Because the main constraints for the design are simplicity and reliability, it was decided that a permanent-magnet generator would be the optimal solution.

While manufacturers for this type on generator were investigated, it was found that they are typically custom-built for specific applications. Future work on this project would include contacting manufacturers to determine the size and cost of a permanent-magnet generator to fit the torque curve of the turbine rotor.

10.6 Braking and Control

In order to govern the rotational speed of the turbine at high wind speeds, a form of braking is required. Several control schemes are available to govern the speed of wind turbines. These include: [26]

- Stall governing: The turbine blades are designed to stall at high wind speeds, reducing torque and therefore rotational speed.
- Active pitch control: The blade pitch is changed using hydraulic or electric actuators to reduce torque at high wind speeds.

- Dynamic (or rheostatic) braking: Power from the generator is routed through a network of resistors, increasing generator torque and reducing rotational speed.

Friction braking is not generally used for speed control because of the large amount of heat that is generated. Advantages and disadvantages of these methods are summarized in the table below:

Table 13: Control methods for wind turbines

Control Method	**Advantages**	**Disadvantages**
Stall Governing	Requires no additional components	Causes reduced power output at lower wind speeds
Active Pitch Control	Does not reduce power output when governing is not required	Requires a complex system of actuators
Dynamic Braking	Does not reduce power output when governing is not required	Requires more complex electrical system and cooling for resistor network

For this application, it was decided that dynamic braking provides an adequate balance between simplicity and performance. Cooling requirements for a rheostatic resistor grid would be reduced in a cold climate. This system would be brought online when the speed of the turbine exceeds 35 revolutions per minute, as measured by a tachometer on the turbine shaft.

Specifying the exact system used is not within the scope of this project. However, research has determined that rheostatic braking has been used successfully on commercially-produced, permanent-magnet generator turbines in the 100 kW range. [27]

For shutdown, cut-out, and emergency stop, mechanical brakes are required. In the wind power industry, externally-contacting drum brakes or disc brakes are commonly used. These are usually spring-applied and mechanically or electrically released. This type of

brake provides the advantage of failing safe, since if power or hydraulic pressure to the braking system is lost, the brakes are automatically applied.

Drum brakes were chosen for the vertical-axis turbine since these can be applied to a simple wear pad on the drive shaft, unlike disc brakes which require that a rotor be mounted to the shaft as well. Multiple braking units would be used, both to provide redundancy and to allow sufficient braking torque to be applied while still using a system that is small enough to be easily removed and replaced if necessary.

While the brake would be applied by spring force, various options are available to release the brakes. These most common types are electromagnetic, hydraulic, and pneumatic release. For this application, electromagnetically-released brakes were chosen since they do not require an external fluid power source. While the turbine will have a compressed air system for starting, pneumatically-released brakes were considered to be unsuitable since this would require a constantly-pressurized compressed gas system, which could pose a serious safety hazard in the case of a failure.

The brakes would be automatically applied when the sustained wind speed is measured by an anemometer to be greater than the turbine's cut-out speed of 94 km/h, or if the rheostatic braking system fails and rotational speed exceeds 35 revolutions per minute for a sustained period. The brakes could also be manually applied to stop the turbine for scheduled maintenance. In a non-emergency shutdown situation, the rheostatic braking system would first be used to reduce speed as much as possible before applying the drum brakes to reduce wear on the drum and pads.

The selection of a specific brake was not within the scope of the project. However, spring-applied, electromagnetically-released drum brakes are readily-available from manufacturers. A typical brake of this type is represented by the TM-I 16 manufactured by SIBRE Siegerland Bremsen GmbH.

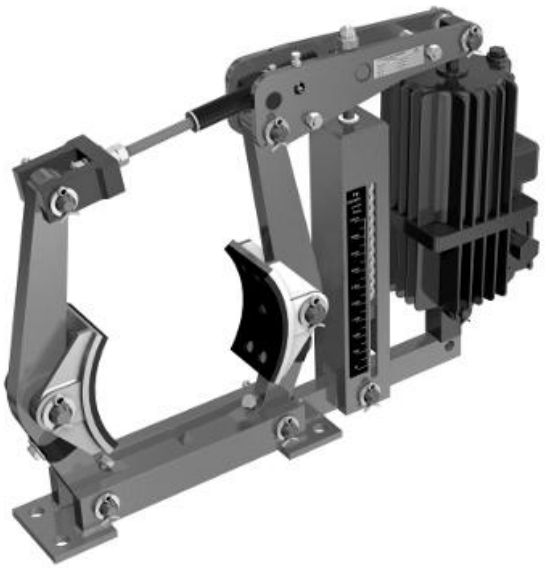

Figure 40: Typical wind turbine drum brake[4]

10.7 Starting

Since H-rotor VAWTs are not self-starting in all conditions [1], an external starting system is required. This can consist simply of back-driving the generator as a motor. However, this system requires a more complex electrical system. For this reason, the alternative of a compressed-air starting system was investigated. Compressed-air starters are commonly used to start large diesel engines and gas turbines, and may be adaptable to vertical-axis wind turbines.

To determine the required staring torque and power, the inertia of the rotating turbine components was computed. Aerodynamic analysis showed that a rotational speed of 1 revolution per minute was sufficient to start the turbine. The torque and power required to spin up the turbine to speed in a time period of five seconds was calculated. The results of this calculation are summarized in the table below:

[4] *Image Credit: SIBRE Siegerland Bremsen GmbH*

Parameter	Result	Unit
Mass Moment of Inertia	1 144 000	kg-m^2
Starting Speed	1	rev/min
Starting Time	5	seconds
Starting Torque	20 910	N-m
Starting Power	4.18	kW
Starting Energy	0.0058	kWh

In contrast to diesel engines and gas turbines, which require a high-speed, low-torque starting system, the wind turbine requires a high-torque, low-speed starter. However, it is reasonable to imagine that a custom-built air starter could be used for the turbine. Alternatively, an off-the-shelf starter with a gear reduction could be used.

The calculations show that the energy required to start the turbine is not significant. This energy would be recovered in 0.2 seconds of operation at the rated wind speed.

An air-starting system would provide the advantage of a simpler electrical system, but would require an external compressor and air receiver. Further investigation is required to determine the relative costs of electric versus compressed-air starting; however, it can tentatively be stated that a compressed-air starting system is a viable option for vertical-axis wind turbines if a simplified electrical system is desired.

11 Economic Analysis

The cost estimates in this report are extrapolations from the economic analysis of Northwind 100, the 100kW wind turbine used by Nalcor in Ramea, Newfoundland, and the diesel generators in Nain, Labrador. [28] [29] The VAWT capital estimate was extrapolated due to the lack of response from venders. These values are fairly accurate because the size of the turbines are relatively similar. The Northwind 100 was broken down in to costs per component and therefore MUN VAWT Design removed unnecessary components such as the yawing system to produce a more appropriate cost estimate for this application. In

addition to the removal of the yawing system, the height of the tower was reduced which significantly reduces the capital cost of the turbine. Using engineering economic principles, the monetary values for maintenance costs, fuel consumption and capital costs were translated through time with an interest rate of 3.5% using the equation below:

Equation 33: Inflation Rate

$$F = P\,(1 + i)^n$$

Where F is the monetary or accumulated value at a future point in time, P is the current or principal value, i is the interest rate and n is the number of years or interest periods between the present and future.

The following findings are estimates only because transportation of diesel and the VAWT are heavily dependent on the community's location and therefore were omitted from this analysis.

Table 14: Key economic estimates

Estimated Capital Cost	$425 000.00
Maintenance Cost/Year - Turbine	$10 000.00
Maintenance Cost/Year – Diesel Generator	$20 000.00
Fuel Cost for 2015	$3 630 967.00
Payoff Period for a Single Turbine	3 years
Payoff Period for an Installation of 5 Turbines	3 years
Payoff Period for an Installation of 20 Turbines	3 years
Payoff Period for an Installation of 50 Turbines	4 years

An initial installation of five turbines will produce sufficient power to reduce annual fuel costs by approximately $1 000 000. This corresponds to a saving of 18% of the total cost of power generation in the target location.

12 Environment

Based on the feedback from phase one of the project MUN VAWT Design decided to investigate the impact of wind turbines on the avian population to assuage the fears raised by many people. A 2001 investigation into the causes of avian collision mortality in the United States estimated that wind turbines accounted for only 0.01 to 0.02% of the total fatalities. [30] More recently, a 2013 Canadian study estimated that the average number of avian deaths per turbine was 8.2 ± 1.4. However, it found this was heavily dependent on location has the average ranged from 0 to 26.9 deaths per turbine. [31]

With this in mind, Nain, the location previously discussed as an area of interest was investigated for potential avian impacts on a proposed wind turbine project. By reading Environmental Assessment's for two different wind turbine project's proposed for Nain in the past it was found that Nain is designated an Important Bird Area (IBA). However this title carries no legal repercussions and Nain is therefore not a legally protected Ecological Reserve. An IBA is an area that meets the requirement set out by the IBA program for monitoring and designation of important areas for the conservation of birds. [32] It was also found that there are 8 Peregrine Falcon, which are considered a threatened species, nests in the surrounding area of Nain. Due to this a 1 km radius around the nest sites was proposed as a buffer zone. [33] The last consideration found was a condition on the release of the project from Governmental review mandating that an avian monitoring program be developed in line with Environment Canada regulations. [34]

13 Project Management

With the completion of the project it is important to highlight where goals were met, exceeded, or fell short of expectations. As per the Gantt chart, all objectives were achieved; however, there were areas where follow-up is required to complete this project. These shortfalls were caused by unforeseen factors such as computational limitations. Three-dimensional CFD modeling was attempted but was unable to be completed due to these limitations. Detailed design such as welding, bolted/flanged connections was not

completed due to the focus on designing the main structural and mechanical components to achieve design life and meet the required standards under all operating conditions. The economic analysis was representative instead of complete because of the lack of response from venders and manufacturers. From a management viewpoint, the scope of this project was larger than anticipated by team members. MUN VAWT Design worked diligently to complete the deliverables set out in the scope for this project and is proud of the work accomplished. The Gantt chart for the project can be found in Appendix E.

14 Future Work

To continue this project to the next stages of development a few steps must be completed. Firstly, a full 3D CFD analysis must be performed to meet the standard requirements. This analysis is very computationally intensive and couldn't be completed with the resources available to MUN VAWT Design. Secondly, a full structural dynamic model should be produced with detailed design analysis into connections. This is also a requirement to complete testing for the standard presented in this report. Engineering outside the scope of this project such as foundation design, civil work and control systems are required. Lastly, full scale testing of the turbine should be completed prior to marketing the product.

15 Summary of Design

The exterior and interior of the turbine is graphically presented below, with highlights and specifications of the key components.

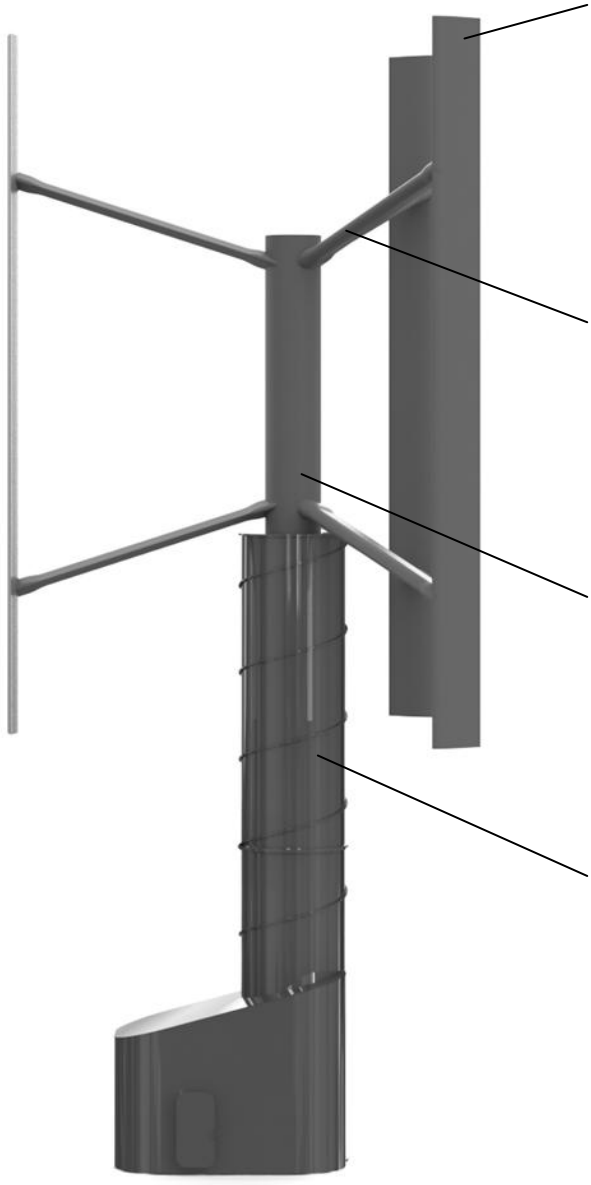

Blades: (x3)
- DU-6-W-200 airfoil
- Chord: 1.6 metres
- Length: 20 metres
- Hollow cross-section with structural ribs
- E-glass fibre / epoxy composite

Struts: (x6)
- Diameter: 0.36 metres
- Wall thickness: 40 mm
- Length: 7.6 metres
- AISI 1045 tubular steel w/ fibreglass aerodynamic fairing

Hub:
- Diameter: 0.6 metres
- Wall thickness: 25 mm
- Length: 8.5 metres
- AISI 1045 tubular steel w/ fibreglass protective fairing

Tower:
- Diameter: 3.0 metres
- Wall thickness: 50 mm
- Height: 15.8 metres (composed of two 7.9-metre sections)
- A35 structural steel
- Helical strake to mitigate vortex-induced vibrations

Figure 41: Exterior of turbine

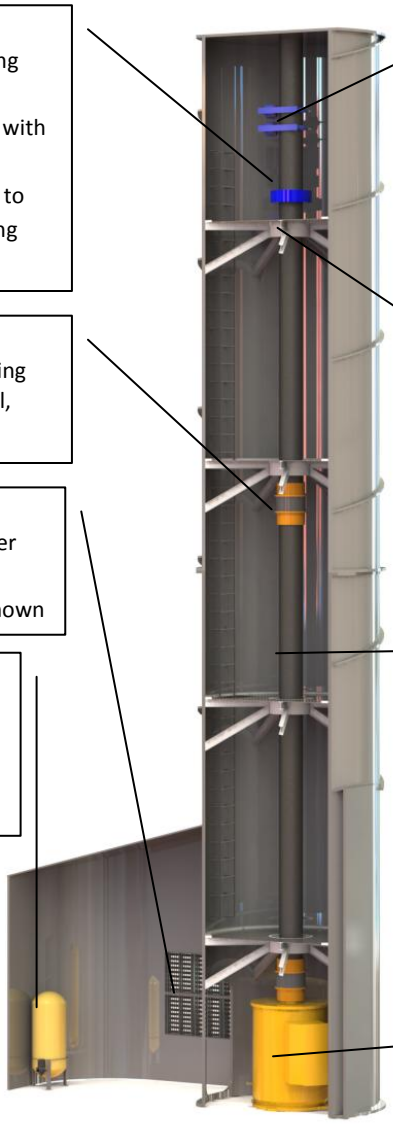

Starting Air Turbine:
- Compressed air starting system
- Coupled to driveshaft with gear reduction
- Located high in tower to reduce shaft flex during starting

Shaft Couplings: (x2)
- Renold RB Flex Coupling
- Allows for axial, radial, and angular

Rheostatic Braking Grid:
- Network of high-power resistors
- Cooling system not shown

Air Receiver & Compressor:
- Supplies compressed air to starting system
- Connection to starter not shown

Shutdown / E-Stop Brakes:
- Spring applied, electromagnetically released
- External-contact drum brakes
- Fails safe
- Located high in tower to reduce shaft deflection during braking

Driveshaft Bearings: (x5)
- Bore: 406.4 mm
- Steel tapered roller bearings
- Low-temperature grease lubrication
- Sockets located in centre of work platforms

Driveshaft:
- Diameter: 406.4 mm
- Wall thickness: 25.4 mm
- Length: 15.8 metres (composed of two 7.9 metre sections)
- AISI 4340 tubular steel
- Fatigue life: Infinite (factor of safety 1.15)
- Connection to hub not shown

Generator:
- Low-speed permanent-magnet generator
- Maximum power: 130 kW
- Operating range: 0 – 35 RPM
- Electrical equipment required for grid connection not shown

Figure 42: Interior of turbine tower

16 Conclusion

The goal of this project was to design a vertical-axis wind turbine with at least 100 kW nameplate capacity for use in remote communities. Key aspects of the design were investigated, including aerodynamics, structural design, vibrational analysis, and mechanical component design. Consideration was also given to non-technical factors; compliance with existing standards, environmental concerns, and an economic analysis were considered to ensure a well-rounded, socially-responsible design. While some further work is required, overall the project met its goals and showed that a robust, long-lifetime VAWT capable of standing up to the harsh weather conditions in Newfoundland and Labrador and across Canada is a feasible endeavour.

Bibliography

[1] E. D. Berg, D. T. Ashwill and J. H. Sutherland, "A Retrospective of VAWT Design," Albuquerque, 2012.

[2] H. Dumitrescu, V. Cardos, A. Dumitrache and F. Frunzulica, "Low Frequency Noise Prediction of Vertical Axis Wind Turbines," The Publishing House of the Romanian Academy, 2010.

[3] D. A. Spera and T. R. Richards, "Modified Power Law Equations For Vertical Wind Profiles," US National Aeronatics and Space Administration, 1979.

[4] Environment Canada, "Historical Climate Data," [Online]. Available: http://climate.weather.gc.ca/. [Accessed 2014 January 2014].

[5] M. T. Iqbal, "A feasibility study of a zero energy home in Newfoundland," Pergamon, St. John's, 2003.

[6] P. Gipe, "News & Articles on Household-Size (Small) Wind Turbines," 7 Feburary 2013. [Online]. Available: http://www.wind-works.org/cms/index.php?id=64&tx_ttnews%5Btt_news%5D=2194&cHash=d1b21f3bd1f35d9e4804f1598b27bd86. [Accessed 5 Feburary 2014].

[7] M. C. Claessens, "The Design and Testing of Airfoils for Application in Small Vertical Axis Wind Turbines," 2009.

[8] P. Sabaeifard, H. Razzaghi and A. Forouzandeh, "Determination of Vertical Axis Wind Turbines Optimal Configuration through CFD Simulations," IACSIT Press, Singapore, 2012.

[9] International Electrotechnical Commision, *IEC 61400-1, Edition 3.0, 2005-08,* 2005.

[10] J. F. Manwell, J. G. McGowan and A. L. Rogers, Wind Energy Explained: Theory, Design and Application, John Wiley & Sons, 2010.

[11] D. Marten and J. Wendler, "QBlade Guidelines v0.6," Technische Universität Berlin, Berlin, 2013.

[12] D. Marten and J. Wendler, *QBlade Guidelines v0.6,* Berlin: Technische Universität Berlin, 2013.

[13] S. Eriksson, H. Bernhoff and M. Leijon, "Evaluation of different turbine concepts for wind power," Swedish Centre for Renewable Electric Energy Conversion, Uppsala, 2006.

[14] A. Shires, "Development and Evaluation of an Aerodynamic Model for a Novel Vertical Axis Wind Turbine Concept," Cranfield University School of Engineering, Cranfield, 2013.

[15] D. Fowley, Fundamentals of Heat and Mass Transfer: Seventh Edition, Jefferson City: John Wiley&Sons, Inc., 2011.

[16] ANSYS Incorporated, *CFX User's Guide,* 2014.

[17] P. J. Gawthrop and G. P. Bevan, "Bond-Graph Modeling," *IEEE Control Systems Magazine,* pp. 24-45, April 2007.

[18] Controllab Products B.V, *20-Sim Reference V4.3,* 2013.

[19] D. S. Nakhla, *Failure Prediction - Primary Design Resources.*

[20] MatWeb LLC.

[21] *Personal communication with Dr. Samer Nakhla,* 28 February 2014.

[22] P. J. Pritchard, Fox and McDonald's Inctroduction to Fluid Mechanics, 8th Edition, Hoboken, NJ, United States: John Wiley & Sons, 2011.

[23] S. S. Rao, Mechanical Vibrations, 5th Edition, Pearson Education Incorporated, 2011.

[24] R. G. Budynas and J. K. Nisbett, Shigley's Mechanical Engineering Design, Ninth Edition, New York, NY, United States: McGraw-Hill, 2011.

[25] W. Wu, V. S. Ramsden, T. Crawford and G. Hill, "A Low-Speed, High-Torque, Direct-Drive Permanent Magnet Generator for Wind Turbines".

[26] National Instruments, "Wind Turbine Control Methods".

[27] Northern Power Systems, *Northern Power 100-21 Spec Sheet.*

[28] Newfoundland & Labrador Hydro, "Additions to Accommodate Load Growth - Isolated Generating Stations," 2012.

[29] Newfoundland & Labrador Hydro, "Preliminary Assesment of Alternative Energy Potential in Coastal Labrador," 2009.

[30] W. P. Erickson, G. D. Johnson, M. D. Strickland, D. P. Young, K. J. Sernka and R. E. Good, "Avian Collisions wiith Wind Turbines: A Summary of Existing Studies and Comparisons to Other Sources of Avian Collision Mortality in the United States," National Wind Coordinating Committee, 2001.

[31] J. R. Zimmerling, A. C. Pomeroy, M. V. d'Entremont and C. M. Francis, "Canadian Estimate of Bird Mortality Due to Collisions and Direct Habitat Loss Associated with Wind Turbine Developments," vol. 8, no. 2, 2013.

[32] Westenwind nv, "Environmental Registration; Nain," 2003.

[33] Unity Bay Energy Limited, "Environmental Assessment Registration; 750 kW Wind Turbine Farm; Nain, Labrador," 2003.

[34] Newfoundland & Labrador Department of Environment, "Environmental Assessment Bulletin," 2003.

[35] California Energy and Power, "Research and Development," California Energy and Power, 2014. [Online]. Available: http://cal-epower.com/research.asp. [Accessed 15 January 2014].

Appendix A: Abbreviations used in IEC 61400-1

The following abbreviations are used in Table 2:

DLC	Design load case
ECD	Extreme coherent gust with direction change
EDC	Extreme direction change
EOG	Extreme operating gust
EWM	Extreme wind speed model
EWS	Extreme wind shear
NTM	Normal turbulence model
ETM	Extreme turbulence model
NWP	Normal wind profile model
Vr+_2	Sensitivity to all wind speeds in the range shall be analysed
F	Fatigue
U	Ultimate strength
N	Normal
A	Abnormal
T	Transport and erection
*	Partial safety for fatigue

Appendix B: Constants used in Bond Graph Model

T_{wind} Equation Constants

A1 = 1.3562E-09;
A2 = -0.000000152;
A3 = 3.7047E-06;
A4 = -0.000018875;
B1 = -1.6095E-07;
B2 = 0.000021514;
B3 = -0.00055922;
B4 = 0.0029273;
C1 = 5.6556E-06;
C2 = -0.0011605;
C3 = 0.033599;
C4 = -0.18318;
D1 = 0.000037268;
D2 = 0.027913;
D3 = -1.0068;
D4 = 5.8732;
E1 = -0.0071703;
E2 = -0.19588;
E3 = 15.044;
E4 = -100.37;
F1 = 0.18113;
F2 = -3.6395;
F3 = -84.52;
F4 = 838.97;
G1 = -1.9004;
G2 = 71.757;
G3 = -264.91;
G4 = -2246.8;
H1 = 7.9895;
H2 = -374.72;
H3 = 3726.9;
H4 = -5058.9;
I1 = -9.8801;
I2 = 500.94;
I3 = -6203.2;
I4 = 16155;

Bond Graph Parameters

I = 1 000 000, Turbine Inertia

R = 0.0018, Bearing Friction

C = 3 960 920, Drive Shaft Stiffness

Appendix C: Excerpt from IEC 61400-1 2007

The wind regime for load and safety considerations is divided into the normal wind conditions, which will occur frequently during normal operation of a wind turbine, and the extreme wind conditions that are defined as having a 1-year or 50-year recurrence period.

The wind conditions include a constant mean flow combined, in many cases, with either a varying deterministic gust profile or with turbulence. In all cases, the influence of an inclination of the mean flow with respect to a horizontal plane of up to 8° shall be considered. This flow inclination angle shall be assumed to be invariant with height.

The expression "turbulence" denotes random variations in the wind velocity from 10 min. averages. The turbulence model, when used, shall include the effects of varying wind speed, shears and direction and allow rotational sampling through varying shears. The three vector components of the turbulent wind velocity are defined as:

– longitudinal – along the direction of the mean wind velocity;
– lateral – horizontal and normal to the longitudinal direction, and
– upward – normal to both the longitudinal and lateral directions, i.e. tilted from the vertical by the mean flow inclination angle.

For the standard wind turbine classes, the random wind velocity field for the turbulence models shall satisfy the following requirements:

a) the turbulence standard deviation, σ_1, with values given in the following subclauses, shall be assumed to be invariant with height. The components normal to the mean wind direction shall have the following minimum standard deviations[3]:
   – lateral component – $\sigma_2 \geq 0{,}7\sigma_1$
   – upward component – $\sigma_3 \geq 0{,}5\sigma_1$
b) the longitudinal turbulence scale parameter, Λ_1, at hub height z shall be given by

$$\Lambda_1 = \begin{cases} 0{,}7\,z & z \leq 60\,m \\ 42\,m & z \geq 60\,m \end{cases} \quad (5)$$

   The power spectral densities of the three orthogonal components, $S_1(f)$, $S_2(f)$, and $S_3(f)$ shall asymptotically approach the following forms as the frequency in the inertial sub-range increases:

$$S_1(f) = 0{,}05\sigma_1^2(\Lambda_1 / V_{hub})^{-2/3} f^{-5/3} \quad (6)$$

$$S_2(f) = S_3(f) = \tfrac{4}{3} S_1(f) \quad (7)$$

c) a recognized model for the coherence, defined as the magnitude of the co-spectrum divided by the auto-spectrum for the longitudinal velocity components at spatially separated points in a plane normal to the longitudinal direction, shall be used.

The recommended turbulence model that satisfies these requirements is the Mann uniform shear turbulence model in Annex B. Another frequently used model that satisfy these requirements is also given in Annex B. Other models should be used with caution, as the choice may affect the loads significantly.

---

3 The actual values may depend on the choice of turbulence model and the requirements in b).

6.3.1 Normal wind conditions

6.3.1.1 Wind speed distribution

The wind speed distribution is significant for wind turbine design because it determines the frequency of occurrence of individual load conditions for the normal design situations. The mean value of the wind speed over a time period of 10 min shall be assumed to follow a Rayleigh distribution at hub height given by

$$P_R(V_{hub}) = 1 - \exp\left[-\pi (V_{hub} / 2V_{ave})^2\right] \quad (8)$$

where, in the standard wind turbine classes, V_{ave} shall be chosen as

$$V_{ave} = 0,2\ V_{ref} \quad (9)$$

6.3.1.2 The normal wind profile model (NWP)

The wind profile, $V(z)$, denotes the average wind speed as a function of height, z, above the ground. In the case of the standard wind turbine classes, the normal wind speed profile shall be given by the power law:

$$V(z) = V_{hub}\left(z / z_{hub}\right)^{\alpha} \quad (10)$$

The power law exponent, α, shall be assumed to be 0,2.

The assumed wind profile is used to define the average vertical wind shear across the rotor swept area.

6.3.1.3 Normal turbulence model (NTM)

For the normal turbulence model, the representative value of the turbulence standard deviation, σ_1, shall be given by the 90 % quantile[4] for the given hub height wind speed. This value for the standard wind turbine classes shall be given by

$$\sigma_1 = I_{ref}(0,75V_{hub} + b); \quad b = 5,6\ \text{m/s} \quad (11)$$

Values for the turbulence standard deviation σ_1 and the turbulence intensity σ_1/V_{hub} are shown in Figures 1a and 1b.

Values for I_{ref} are given in Table 1.

---

4 Note, if other quantiles are desired for additional optional load calculations, they may be approximated for the standard classes by assuming a log-normal distribution and

$E\langle\sigma_1|V_{hub}\rangle = I_{ref}(0,75V_{hub} + c);\ c = 3,8\ \text{m/s}$

$Var\langle\sigma_1|V_{hub}\rangle = (I_{ref}(1,4\ \text{m/s}))^2$

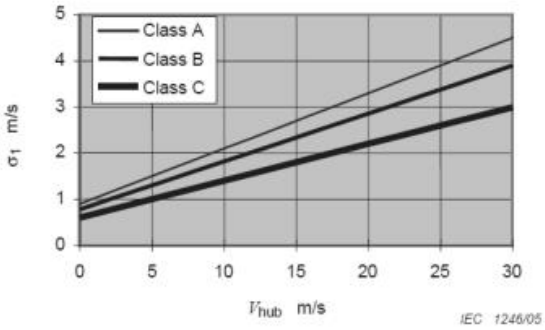

Figure 1a –Turbulence standard deviation for the normal turbulence model (NTM)

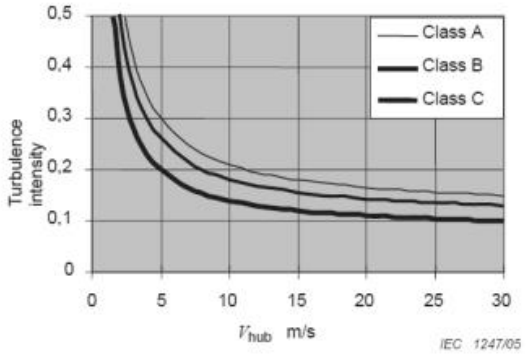

Figure 1b – Turbulence intensity for the normal turbulence model (NTM)

Figure 1 – Normal turbulence model (NTM)

6.3.2 Extreme wind conditions

The extreme wind conditions include wind shear events, as well as peak wind speeds due to storms and rapid changes in wind speed and direction.

6.3.2.1 Extreme wind speed model (EWM)

The EWM shall be either a steady or a turbulent wind model. The wind models shall be based on the reference wind speed, V_{ref}, and a fixed turbulence standard deviation, σ_1.

For the steady extreme wind model, the extreme wind speed, V_{e50}, with a recurrence period of 50 years, and the extreme wind speed, V_{e1}, with a recurrence period of 1 year, shall be computed as a function of height, z, using the following equations:

$$V_{e50}(z) = 1.4 V_{ref} \left(z / z_{hub} \right)^{0.11} \quad (12)$$

and $V_{e1}(z) = 0.8 V_{e50}(z)$ (13)

In the steady extreme wind model, allowance for short-term deviations from the mean wind direction shall be made by assuming constant yaw misalignment in the range of ±15°.

For the turbulent extreme wind speed model, the 10 min average wind speeds as functions of z with recurrence periods of 50 years and 1 year, respectively, shall be given by

$$V_{50}(z) = V_{ref}(z/z_{hub})^{0,11} \quad (14)$$

$$V_1(z) = 0,8V_{50}(z) \quad (15)$$

The longitudinal turbulence standard deviation[5] shall be:

$$\sigma_1 = 0,11V_{hub} \quad (16)$$

6.3.2.2 Extreme operating gust (EOG)

The hub height gust magnitude V_{gust}[6] shall be given for the standard wind turbine classes by the following relationship:

$$V_{gust} = \text{Min}\left\{1,35(V_{e1} - V_{hub});\ \ 3,3\left(\frac{\sigma_1}{1+0,1(\frac{D}{\Lambda_1})}\right)\right\} \quad (17)$$

where

σ_1 is given in equation (11);

Λ_1 is the turbulence scale parameter, according to equation (5);

D is the rotor diameter.

The wind speed shall be defined by the equation:

$$V(z,t) = \begin{cases} V(z) - 0,37V_{gust}\sin(3\pi t/T)(1-\cos(2\pi t/T)) & \text{for } 0 \le t \le T \\ V(z) & \text{otherwise} \end{cases} \quad (18)$$

where

$V(z)$ is defined in equation (10)

T = 10,5 s.

An example of the extreme operating gust (V_{hub} = 25 m/s, Class I_A, D = 42 m) is shown in Figure 2:

---

5 The turbulence standard deviation for the turbulent extreme wind model is not related to the normal (NTM) or the extreme turbulence model (ETM). The steady extreme wind model is related to the turbulent extreme wind model by a peak factor of approximately 3,5.

6 The gust magnitude was calibrated to together with the probability of an operation event such as starts and stops to give a recurrence period of 50 years.

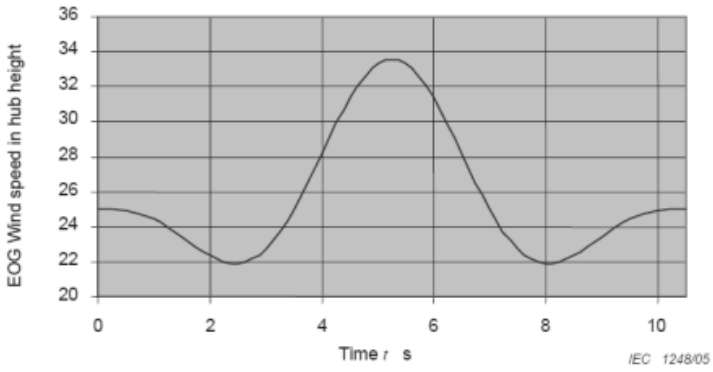

Figure 2 – Example of extreme operating gust

6.3.2.3 Extreme turbulence model (ETM)

The extreme turbulence model shall use the normal wind profile model in 6.3.1.2 and turbulence with longitudinal component standard deviation given by

$$\sigma_1 = c \quad I_{\text{ref}}\left(0.072\left(\frac{V_{\text{ave}}}{c}+3\right)\left(\frac{V_{\text{hub}}}{c}-4\right)+10\right);\ c = 2 \text{ m/s.} \tag{19}$$

6.3.2.4 Extreme direction change (EDC)

The extreme direction change magnitude, θ_e, shall be calculated using the following relationship:

$$\theta_e = \pm 4 \arctan\left(\frac{\sigma_1}{V_{\text{hub}}\left(1+0.1\left(\frac{D}{\Lambda_1}\right)\right)}\right) \tag{20}$$

where

σ_1 is given by equation (11) for the NTM;

θ_e is limited to the interval ±180°;

Λ_1 is the turbulence scale parameter, according to equation (5); and

D is the rotor diameter.

The extreme direction change transient, $\theta(t)$, shall be given by

$$\theta(t) = \begin{cases} 0^\circ & \text{for} \quad t < 0 \\ \pm 0.5\theta_e(1-\cos(\pi t/T)) & \text{for} \quad 0 \le t \le T \\ \theta_e & \text{for} \quad t > T \end{cases} \tag{21}$$

where T = 6 s is the duration of the extreme direction change. The sign shall be chosen so that the worst transient loading occurs. At the end of the direction change transient, the direction is assumed to remain unchanged. The wind speed shall follow the normal wind profile model in 6.3.1.2.

Appendix D: Airfoil Bending Moment Calculations

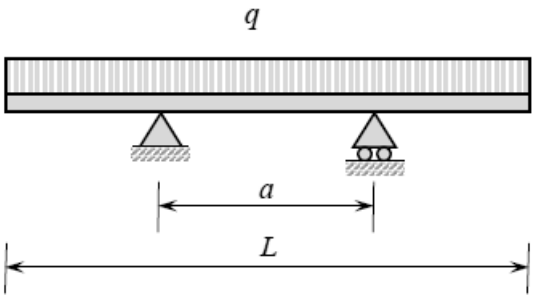

By inspection, the maximum bending moments will occur at the supports and at the mid-span.

Moment at Supports:

$$M_{sup} = \frac{q}{8}L^2\left(1-\frac{a}{L}\right)^2$$

Moment at Mid-span:

$$M_{mid} = \frac{q}{4}L^2\left(\frac{a}{L}-\frac{1}{2}\right)$$

Equating the two:

$$\frac{q}{8}L^2\left(1-\frac{a}{L}\right)^2 = \frac{q}{4}L^2\left(\frac{a}{L}-\frac{1}{2}\right)$$

Negating the coefficients q and L and expanding:

$$\left(\frac{1}{2}-\frac{a}{L}+\frac{a^2}{2L^2}\right) = \left(\frac{a}{L}-\frac{1}{2}\right)$$

$$\left(1-2\frac{a}{L}+\frac{a^2}{2L^2}\right) = 0$$

$$\frac{a}{L} = 0.585786 \; or \; \frac{a}{L} = 3.41421$$

Since the supports cannot be spaced farther apart than the blade is long, $\frac{a}{L} = 0.586$ is the optimal support spacing. Either bending moment formula can then be used to calculate maximum bending moment.

Appendix E: Gantt Chart